Study of Novel Nanoparticle Sensors for Food pH and Water Activity

By Xiang Zhang

A thesis submitted to the

Graduate School-New Brunswick

Rutgers, The State University of New Jersey

in partial fulfillment of the requirements

for the degree of

Master of Science

Graduate Program in Food Science

Written under the direction of

Professor Richard D. Ludescher

and approved by

_____

_____

_____

New Brunswick, New Jersey

October, 2009

ABSTRACT OF THE THESIS

Study of Novel Nanoparticle Sensors for Food pH and Water Activity

By Xiang Zhang

Thesis Director: Professor Richard D. Ludescher

Food sensors, sensitive to food properties, including temperature, oxygen, moisture content and pH, are used in food processing and other food related fields. Recently, applying sensor technology in the food industry has been further emphasized. Nanoparticles, with diameters of tens to hundreds of nanometers, also have generated considerable interest as sensors because of their small size and related novel characters. In this study, we developed fluorescent sensors for food pH based on nanoparticles and investigated water activity probes.

The nanoparticles, fabricated from food grade starch and gelatin with dimensions of ~20-50 nm, were doped with three pH-sensitive probes. Quinine and harmane were non-covalently attached onto starch nanoparticles, while gelatin nanoparticles were covalently labeled with fluorescein isothiocyanate (FITC). The study of labeled nanoparticle sensors in buffer solutions of varying pH's showed the correlation between pH and emission spectra. Quinine labeled starch nanoparticle (QSNP) sensors exhibited blue shifts of emission spectra as pH increased; the ratio of peak intensity or peak area of emission spectra at two different emission wavelengths also decreased dramatically in the range of pH~3.0-5.0. Harmane labeled starch nanoparticle (HSNP) sensors and FITC

labeled gelatin nanoparticle (FGNP) sensors did not present any emission spectra shifts. However, the former's ratio of peak intensity or peak area increased as pH increased in the range of pH~7.0-9.0; the latter's decreased as pH increased in the range of pH~2.5-7.5. Moreover, FGNP sensors were applied in different real food products. Comparing actual food pH with calculated sensor pH based on a calibration curve suggested that using FGNP sensors to detect food pH is accurate (~1-5% error). Duplicated fluorescent tests of FGNP sensors also showed good reproducibility. These results support a new methodology of using nanoscopic sensors for the measurement of food pH.

Study of water activity was focused on charactering the probes Prodan and Laurdan. Prodan was investigated in different saturated salt solutions and water-glycerol solution systems; Laurdan was investigated only in saturated salt solutions. However, these studies did not show any expected correlation between water activity and emission spectra shifts. Therefore, Prodan and Laurdan may not be good indicators of water activity

Acknowledgement

I would sincerely like to thank my advisor Dr. Richard Ludescher for all his support when I transferred from chemistry department to food science department. I am very grateful to him for providing me such a wonderful opportunity to study in this new field and do the research I am interested in. His guidance inspired me, making this research much easier for me to complete.

I would like to thank Dr. Qingrong Huang for providing his lab equipment for some experiment and valuable guidance on nanoparticles. I would also like to thank Dr. Paul Takhistov for serving on my committee.

I would specially thank my lab mates, Yumin, Kasi, Tom, Rashimi, Sanaz, Andrew, Brandon, Xiaotian for the great environment in the lab. My experiment was much easier with all the help and support from you all. I also would like to thank all my friends in food science building. Thanks for your guidance and helping me use different kinds of instrument.

At last, I would thank my family, my mom and dad. Thank you for your support and encouragement in the past three years. When I transferred, when I was looking for a job, you were always standing with me and providing all the confidence and belief that I needed. Thank you so much.

Table of Contents

Lists of Tables

List of illustrations

Chapter 1: Introduction

Introduction

Food sensors

Used in food processing and other food related fields, food sensors are sensitive to properties of foods, such as analytical or physical properties including temperature, oxygen, moisture content, pH, microbes and so on. They must be accurate and sensitive and, hopefully, will also be rapid, inexpensive, and easy to use. The use of food sensors has a long history. A good example is the thermometer, a food sensor for temperature. It appeared in the 17^{th} century and has been widely used to monitor the temperature of a stock room or refrigerator over the centuries. As more and more chemical and biological recognition strategies with ultra sensitive electrical, magnetic or optical detection schemes developed, although the issue of food quality and safety has still dominated the food industry, recent trends have further emphasized the importance of applying new and advanced sensor technology in the food industry.

The following brief summary of recent reports illustrate that the applications of food sensors in food lab research and food industry are very extensive. Shape memory polymers are used in frozen preservation of food as a sensor reflecting the temperature (Kondo et al., 1991). Optical sensors monitor the oxygen content in foods packaged under modified atmosphere (Mills, 2005; O'Mahony et al., 2005). Synthetic multifunctional pores with the assistance of enzyme as co-sensors serve as sugar concentration sensors in soft drinks (Litvinchuk et al., 2005). Catalytic nanoparticles of Y_2O_3 with chemiluminescence detect

trimethyl amines in fish (Zhang et al., 2005). The food sensor list goes far beyond these listed above and is still in rapid development driven by industry need, new instrument and sensor development.

Nanoparticle sensors

Nanoparticles, with diameters of tens to hundreds of nanometers, have some novel optical, magnetic and electronic properties and generate considerable interest as sensors in many fields. A recent example of applying nanoparticle sensors in food is using biofunctionalized magnetic nanoparticles with integrated mid-infrared pathogen sensor to isolate particular bacteria from food matrixes (Ravindranath et al., 2009). In this case, nanoparticles' detectable property is changed after biofunctionalization, which gives these nanoparticles new analytical characters. This is one of the main analytical reasons why functional nanoparticles are thus attractive as sensors for scientists.

The other reason making nanoparticles so attractive to scientists is their high surface/volume ratio, which is directly related to their small size. Recent research using nanoparticles as part of a drug delivery system showed that nanoparticles were able to adsorb high antibiotic amounts due to their high surface/volume ratio (Fernanda et al., 2009). Based on this feature, nanoparticles as sensors can be expected to provide high signal/noise ratio as they are able to adsorb or be labeled with more probes.

Other applications of nanoparticle sensors in foods include (but are not limited to): agar-embedded nanoparticles comprising phospholipids and chromatic polymer monitor bacterial contaminations in foods and bacterial antibiotic resistance by color and fluorescence changes of chromatic transitions (Silbert et al., 2006); gold nanoparticles conjugated with thermoresponsive copolymer sensing thiol to determine cysteine by blue-to-red chromatic change (Shimada et al., 2007); gold nanoparticle-modified electrodes determine the carbohydrate inulin in foods (Manso et al., 2008).

Luminescent nanoparticles

Luminescence techniques are versatile and can provide extreme sensitivity, thus are widely employed in nanoparticle sensors (Liang et al., 2005). Luminous nanoparticles can be either intrinsic or extrinsic. The former group is nanoparticles composed of a luminescent material, including individual spin-coated Ag nanoparticles (Maali et al., 2003), biodegradable luminescent porous silicon nanoparticles (Park et al., 2009), nanocrystalline semiconductors (quantum dots) (Murphy, 2002) and so on. The latter group is nanoparticles labeled with a luminescent chromophore. Examples include multiporphyrin-modified CdSe nanoparticles (Kang et al., 2008), texas red or fluorescein amine doped gelatin nanoparticles (Coester et al., 2000), and lanthanide ion doped silica nanoparticles (Hai et al., 2004).

The luminous nanoparticles developed in this work will be extrinsic and be labeled with organic chromophores. There are some distinct analytical advantages to using fluorescent nanoparticles rather than using chromophores directly. First, as discussed above, nanoparticles can be loaded with large number of individual chromophores depending on their size and doping level, and thus can be much brighter than individual chromophores. Second, researches have proved that chromophores, after being embedded in nanoparticles, often have higher quantum yields and longer lifetimes (Ferrer & Del Monte, 2005; Lian et al., 2004; Wang, Ling et al., 2004), which will further increase their brightness and signal sensitivity. Third, embedded chromophores are protected by nanoparticle frameworks from chemical and photochemical degradation, and thus are more stable (Wang, Wang, et al., 2005; Taylor et al., 2000).

Hydrocolloid nanoparticles

Four hydrocolloid materials, gelatin, starch, chitosan and alginate have been reported that can be readily fabricated into nanoparticles with a diameter ranging from <50 nm to ~250 nm. Previous investigations have been mainly focused on their applications as delivery vehicles for DNA, drugs, nucleic acids and other pharmaceutical agents. However, recently, there are more papers investigating their applications in sensor technology, including preparing fluorescence starch nanoparticles as plant transgenic vehicle (Liu et al., 2008), using electroactive chitosan nanoparticles for single nucleotide polymorphism detection (Kerman et al., 2008) and using pH-sensitive chitosan nanoparticles for oral administration (Zheng et al., 2007).

More information about gelatin and starch is provided below, as these two hydrocolloids were employed in this study.

Gelatin: Gelatin nanoparticles can be generated in two ways, using a water in oil microemulsion technique (Cascone et al., 2002; Gupta et al., 2004) or a two step desolvation technique (Coester et al., 2000; Azarmi et al., 2006). The latter method was extensively investigated and used in this study. The size of nanoparticles produced by two step desolvation technique varies from 20 nm to 200 nm, depending on many factors, including but not limited to temperature, pH, gelatin type, agitation speed, crosslink level, and desolvating agent (Jahanshahi et al., 2008; Azarmi et al., 2006). Because gelatin contains numerous functional groups, many probes can be labeled. Probes can be embedded within gelatin nanoparticles before crosslinking, like fluorescein-labeled dextran (Kommareddy et al., 2005; Gupta et al., 2004), and the non-covalent fuorescent dyes Texas red and fluorescein amine (Coester et al., 2000). Gelatin nanoparticles can also be labeled at surface amino groups by fluorescein isothiocyanate after crosslink (Oppenheim & Stewart, 1979).

Starch: Starch nanoparticles are mainly synthesized by water-in-oil microemulsion method (Wang et al., 2004; Zhai et al., 2008). The range of nanoparticles is from 20 nm to over 100 nm, with most about 40-60 nm (Wang et al., 2004). Many factors, such as surfactant, concentration of starch solution, oil/water volume ratio, sonication and crosslinking level can all affect nanoparticle size. Although the application of labeling starch nanoparticles with fluorescent probes is still limited, starch granules have been non-covalently labeled by

a wide variety of fluorescent dyes, including Calcofluor white (Glenn et al., 1992), acridine orange (Badenhuizen, 1965; Alder et al., 1995), eosin Y (Seguchi, 1986), erythrosin B (Pravinata & Ludescher, 2003) and so on. Among them, some dyes appear to be permanently labeled onto starch albeit in non-covalent manner (Revilla et al., 1986). Since starch is a neutral polymer and least complicated by the presence of acid and base groups, starch nanoparticles may be a very good candidate for developing pH-sensitive fluorescent food sensors.

Potential and advantages of luminescent nanoparticles as food sensors

As mentioned above, nanoparticles have many advantages due to their small size and novel electronic, optical, and magnetic properties. Nanoparticles combined with fluorescent technology would be even more powerful, providing following potential benefits for using nanoparticles as food sensors:

High signal/noise ratio: Nanopartcles with a diameter below 100 nm will have high surface/volume ratio; hence, for gelatin nanoparticles, more surface amino groups will be accessible to be labeled by fluorescent dyes, like fluorescein isothiocyanate. Meanwhile, given that encapsulation in nanoparticles increases the brightness of many chromophores (Ferrer & Del Monte, 2005; Lian et al., 2004; Wang, Ling et al., 2004), no matter where dyes are labeled, labeled at surface or loaded inside, they will always provide signals readily detectable by using inexpensive, hand-held, portable instruments.

Easily dispersible: Both starch nanoparticles and gelatin nanoparticles have been reported that can be easily dispersed in solution. In addition, nanoparticles' small size makes them susceptible to Brownian motion. Once they are dispersed in solution, they will remain dispersed and never settle or cream. Hence, nanoparticles will be suitable to be applied in liquids, emulsions, food ingredients or food matrixes by simply mixing.

Rapid equilibrium: As nanoparticles would be easily dispersible in foods and food matrixes, their nano-scale size would also help them to reach rapid equilibrium with local food properties or local analyte concentration.

Close contact with food matrix and site specific: Nanoparticles are so small that they can be easily dispersed in food matrix and be in intimate contact with food matrix to provide micro-environment information. That information must illustrate the local state of the food matrix in three-dimensions and could even be read by a fluorescence microscope.

Provide specific signal: A lot of information could be provided by luminescent nanoparticles' signals, which include intensity ratios, luminescent lifetimes or energy transfer intensities. Once calibrated, that information can provide unambiguous analytical indicators.

Sensorily neutral: Starch and gelatin nanoparticles can be generated using food grade materials and thus be generally recognized as safe. By using food-safe dyes, it is possible to make luminous starch or gelatin nanoparticles even edible, and then they can be

directly added into food. Their low volatile and use level in food can make them tasteless and odorless; their small size will not modulate the food texture as well.

Versatile yet selective: Both starch and gelatin nanoparticles provide an excellent framework for versatile use. Different dyes can be combined with them, as cited above, to achieve different analytical sensing functions.

In this study, efforts were focused on developing hydrocolloid nanoparticle sensors for *food pH* and *water activity*. Therefore, more background about food pH and water activity and the significance of developing fluorescent nanoparticle sensors for food pH and water activity are provided below.

Food pH

The pH value of food is a direct function of the free hydrogen ions present in that food. Its definition is the negative logarithm value of the activity of dissolved hydrogen ions. It plays an important role in many aspects of foods. First, free hydrogen ions are released by various acids present in foods, which give foods their distinct sour flavor. Second, pH has many affects on food-related chemical reactions, which can further affect food processing and fermentation operations. It will affect salting and dry-cured ham quality (Garcia-Rey et al., 2004), chemical composition and function properties of cheddar cheese and reduced-fat mozzarella cheese (Pastorino et al., 2003; Sheehan et al., 2004). It can also alter caramelization and Maillard reaction kinetics, like controlling the browning rate of high hydrostatic pressure processed mango puree during storage (Guerrero-Beltran et al., 2006 & Ajandouz et al., 1999).Third, pH is important in food preservation as well. Low pH may

inhibit the growth of many microorganisms, like spores of *Clostridium botulinum*, which are hard to kill and may survive for many years but cannot grow if the pH of food is 4.6 or lower. Hence, it provides an alternative approach to preserve foods by acidifying foods to lower pH to inhibit growth of microorganisms.

As pH is so important in many aspects, the development of pH indicators has never stopped. In the 17th century, vegetable dyes such as litmus were used to indicate the acidic and basic properties of solutions (Boyle, 1664; Partington 1961). More recently, pH-sensitive fluorescence indicators also appeared, including mutants of green fluorescent protein (Hess et al., 2004) and fluorescein-labeled silica nanoparticles (Duan et al., 2003). During this exploration, lots of pH-sensitive dyes have been discovered and investigated. In this study, three pH-sensitive dyes were selected to be labeled onto starch or gelatin nanoparticles. They are quinine, harmane and fluorescein isothiocyanate (FITC).

Quinine is a well-characterized pH-dependent fluorophore (Volmar, 1936) and has been applied to measure pH in live cells (Lee & Forte, 1980), in paper (Moorthy et al., 1998) and in microfluidic reactors (Shinokara et al., 2004). Its molar absorptivity changes over the pH interval from 2.5 to 7.0, indicating that quinine is a sensitive indicator of pH over a region especially relevant to food (Morton, 1975). Quinine is also very famous for its effectiveness in curing malaria. Hence, it can be recognized as a food-safe chromophore to be used to develop edible fluorescent nanoparticles.

Harmane is one of the harmala series alkaloids (Wolfbeis & Fürlinger, 1982), which are known to be highly fluorescent and are potent inhibitors of the enzyme manoamine oxidase (Wolfbeis, 1985). Hence, it may not be safe to use harmane in foods. Harmane naturally exists in many plants and can be extracted from plants and cigarette smoke (Wolfbeis et al., 1982). Previous researches have reported that harmane is a useful indicator for determination of pH in the physiological range (Wolfbeis et al., 1982).

FITC is an isothiocyanate derivative of fluorescein. Because of its isothiocyanate reactive group, FITC can easily react with amine and sulphydryl groups and then covalently attach onto protein. FITC is thus widely used in labeling proteins. Previous researches have proved that fluorescein displays four prototropic forms (cation, neutral, monoanion and dianion) in the pH range 1~9 (Yguerabide et al., 1994; Sjöback et al., 1995). As FITC has almost the same structure as fluorescein except for its isothiocyanate group, it makes sense that FITC also displays four prototropic forms in the pH range 1~9 and is as pH-sensitive as fluorescein.

As indicated above, food pH is important not only in microbial growth inhibition, but also in the chemical reactions that occur during food processing, fermentation and storage processes. Precise pH control during food processing operations is highly desirable. Yet, the traditional pH electrode is only suitable for off-line use. Fluorescent nanoparticle sensors, if generated from edible starch or gelatin and labeled with food-safe fluorescent chromophores, could be edible and generally regarded as safe. These edible fluorescent nanoparticle sensors then may be a potential candidate to be added into foods to carry out in-line pH measurement in food processing operations. It would be a huge advantage

compared to conventional pH electrode. In addition, nanoparticle sensors have the ability to provide pH information of small food matrix or anywhere that pH electrode cannot reach. Hence, fluorescent nanoparticle sensors are very attractive and beneficial.

The initial effort of developing such edible fluorescent nanoparticle sensors has been made and three fluorescent nanoparticle sensors were obtained through this study. They are quinine-labeled starch nanoparticle sensors, harmane-labeled starch nanoparticle sensors and FITC-labeled gelatin nanoparticle sensors. They are all tested in various pH buffer solutions to verify their pH-sensitivity and obtain calibration curves. FITC labeled gelatin nanoparticle sensors were even tested in foods and successfully indicated food pH. Although not all of them are edible, this is still a good start and a new method of developing food sensors has been set up. Future work may focus on searching for more food-safe fluorescent probes, label them onto nanoparticles and apply them into real food systems.

Water activity

The direct relationship which often exists between the presence and amount of water in a food and its relative tendency to spoil was first discovered by scientists during the middle and end of the 19th century (Hardman, 1989). However, the thermodynamically correct definition of water activity did not come out until 1976, which is defined as below (Hardman, 1976):

$$a_w = p^{equ} / p^0$$

Where a_w is the water activity, p^{equ} is the partial vapor pressure of water in equilibrium

with the solution and p^0 is the vapor pressure of pure water at the same temperature and pressure as the solution.

Water activity is so important relating to food quality that much research has been done to illustrate its influence in foods. The moisture in the reactions that occur during browning has been investigated for many years. The maximum browning rate in many foods appears to be in the range of 0.40-0.60 a_w, while at very high water contents (>0.95 a_w) moisture may strongly inhibit browning by diluting the reactive species and at low a_w substrates mobility are limited because of lack of water (Labuza & Saltmarch, 1981; Petriella et al., 1985; Chung & Toyomizu, 1976). Nonenzymatic browning reactions can also be affected by water through inhibiting or enhancing some of the intermediate reactions (Labuza & Saltmarch, 1981).

The influence of a_w on lipid oxidation is just opposite to its influence on browning reactions. Autoxidation of lipids occurs rapidly at low a_w conditions and reaches a minimum around 0.3-0.5 a_w because of the "antioxidant effect", which is attributed to bonding of hydroperoxides and hydration of metal catalysts. Further increases in a_w will increase the rate of oxidation, because the mobility of reactants is increased by water (Labuza, 1975; Karel, 1980; Heidelaugh & Karel, 1970).

Water activity will also affect the nutritional quality of foods. Stability of vitamin C in fortified formula foods and stability of vitamin A in wheat flour at various water activities have been investigated (Arya et al., 1990; Sablani et al., 2007). Although different food models may give different results, these results all showed that the rate of vitamin degradation does have a connection with water activity: it may affect the mobility of metal ions or enzymes, which act as catalysts in the deterioration procedure. Because of that, denaturation of most food proteins is also affected by water activity (Hagerdah & Martens, 1976). Some browning-related protein denaturations associate with water activity as well (Labuza & Saltmarch, 1981).

Microbial activity is another important issue in foods and is affected by water activity. There is always a water activity limitation below which groups of microorganisms can no longer reproduce (Troller & Christian, 1978). This feature sometimes can be exploited in food regulations. Examples are the requirement of $a_w<0.85$ for the transportation of dried foods in the US Good Manufacturing Practices regulations (Hardman, 1989).

The last important issue relating to water activity is food texture. People prefer moist, juicy, tender and chewy foods, which require moisture content to play an important role. There is a considerable literature on this topic. Cheese was found to possess a more acceptable texture with a high a_w in the range of 0.90-0.94 (Kreisman & Labuza, 1978). Potato chips showed critical water activity for optimal chip crispness and breaking strength at a_w about 0.4 (Quast & Karel, 1972; Katz & Labuza, 1981). The affect of a_w on food textures is very specific to the kind of food and the suitable a_w for foods vary case by case.

As water activity is so important in food quality, precise control of water activity during food processing and storage is highly desirable. However, current commercial water activity meters, like pH meters, cannot conduct in-line tests. Fluorescent nanoparticle sensors, which can reach rapid equilibrium with environment as discussed above, would be a very good potential solution for rapid in-line use. The question here is first looking for a water activity sensitive probe. Surprisingly, there do not appear to be any applications of fluorescence to monitor water activity. Most research that has been done is focused on the solvent polarity, as fluorescence emission spectra are often sensitive to it. Several probes are involved in these researches, including Laurdan (Salgo et al., 1995; Parasassi et al., 1990, 1994) and Prodan (Krasnowska et al., 1998; Massey, 1998). Their solvent polarity sensitive properties are applied to measure the penetration of water into lipid bilayers. In this study, these two probes are also employed to develop water activity nanoparticle sensors. Their fluorescence emission spectra are expected to present shifts at various water activity conditions compared to pure water.

References

Adler, J., Baldwin, P., Melia, C. (1995) Starch damage. Part 2: types of damage in ball-milled starch, upon hydration observed by confocal microscopy. Starch/ Staerke 47, 252-256.

Ajandouz, E. H., Puigserver, A. (1999) Nonenzymic Browning Reaction of Essential Amino Acids: Effect of pH on Caramelization and Maillard Reaction Kinetics. Journal of Agricultural and Food Chemistry, 47(5), 1786-1793.

Arya, S. S., Thakur, B. R. (1990) Effect of water activity on vitamin A degradation in wheat flour (atta). Journal of Food Processing and Preservation, 14(2), 123-34.

Avila, M., Zougagh, M., Escarpa, A., Rios, A. (2007) Supported liquid membrane-modified piezoelectric flow sensor with molecularly imprinted polymer for the determination of vanillin in food samples Talanta, 72(4), 1362-1369.

Azarmi, S., Huang, Y., Chen, H., McQuarrie, S., Abrams, D., Roa, W., Finlay, W. H., Miller, G. G., Löbenberg, R. (2006) Optimization of a two-step desolvation method for preparing gelatin nanoparticles and cell uptake studies in 143B osteosarcoma cancer cells. J Pharm Pharmaceut Sci 9(1):124-132.

Badenhuizen, N. (1965) Detection of changes in the paracrystalline pattern of starch granules by means of acridine orange. Staerke 17, 69-74.

Boyle, R. (1664) *The Experimental History of Colors.* (As cited in Partington, 1961)

Cascone, M., Lazzeri, L., Carmignani, C., Zhu, Z. (2002) Gelatin nanoparticles produced by a simple W/O emulsion as delivery system for methotrexate. J. Material Sci. Mat. Med. 13, 523-526.

Chung, C. Y. and Toyomizu, M. (1976) Studies on the browning of dehydrated foods as a function of water activity. I. Effect of aw on browning in amino acid-lipid systems. Bull. Jap. Soc. Sci. 42, 697-702

Coester, C. (2003) Development of a new carrier system for oligonucleotides and plasmids based on gelatin nanoparticles. New Drugs 1, 14-17.

Coester, C., Langer, K., Von Briesen, H., Kreuter, J. (2000) Gelatin nanoparticles by two step desolvation—a new preparation method, surface modifications and cell uptake. J. Microencapsulation 17, 187-193.

Duan, J-H., Wang, K-M., He, X-X., Tan, W-H., Liu, B., He, C-M., Mo, Y-Y., Huang, S-S., Li, D. (2003) A novel nano-sensor based on fluorescent core-shell silica nanoparticle for pH measurements in murine macrophages. Hunan Daxue Xuebao, Ziran Kexueban 30, 1-5.

Fernanda, C., Iolanda, F., Mariangela. B., Andrea, M., Lucio, D., Antonella, P. (2009) Antibiotic delivery polyurethanes containing albumin and polyallylamine nanoparticles. European journal of pharmaceutical sciences: official journal of the European Federation for Pharmaceutical Sciences 36(4-5), 555-64.

Ferrer, M., Del Monte, F. (2005) Enhanced emission of Nile red fluorescent nanoparticles embedded in hydrid sol-gel glasses. J. Phys. Chem. B 109, 80-86.

Garcia-Rey, R. M., Garcia-Garrido, J. A., Quiles-Zafra, R., Tapiador, J., Luque de Castro, M. D. (2004) Relationship between pH before salting and dry-cured ham quality. Meat Science 67(4), 625-632.

Glenn, G., Pitts, M., Liao, K., Irving, D. (1992) Block-surface staining for differentiation of starch and cell walls in wheat endosperm. Biotechnic & Histochemistry 67, 88-97.

Guerrero-Beltran, J. A., Barbosa-Canovas, G. V., Moraga-Ballesteros, G., Moraga-Ballesteros, M. J., Swanson, B. G. (2006) Effect of pH and ascorbic acid on high hydrostatic pressure-processed mango puree. Journal of Food Processing and Preservation, 30(5), 582-596.

Gupta, A., Gupta, M., Yarwood, S., Curtis, A. (2004) Effect of cellular uptake of gelatin particles on adhesion, morphology, and cytoskeleton organization of human fibroblasts. J. Controlled Release 95, 197-207.

Hagerdah, B. and Martens, H. (1976) Influence of water contents on the stability of myoglobin to heat treatment. J. Food Sci. 41, 933-937.

Hai, X., Tan, M., Wang, G., Ye, Z., Yuan, J., Matsumoto, K. (2004) Preparation and a time-resolved fluoroimmunoassay application of a new europium fluorescent nanoparticles. Analytical Sciences 20, 245-246.

Hardman, T. M. (1976) Measurement of water activity. Critical appraisal of methods. In: Intermediate Moisture Foods, R. Davis, G. G. Birch and K. J. Parker (Eds), Applied Sci. Pub., London.

Hardman, T. M. (1989) Water and Food Quality, Elsevier Applied Science, London, New York.

Heidelbaugh, N. and Karel, M. (1970) Effects of water binding agents on oxidation of methyl linoleate. J. Am. Oil Chem. Soc. 47, 539.

Hess, S., Heikal, A., Webb, W. (2004) Fluorescence photoconversion kinetics in novel green fluorescent protein pH sensors (pHlurions). J. Phys. Chem. B 1008, 10138-10148.

Jahanshahi, M., Sanati, M. H., Hajizadeh, S., Babaei, Z. (2008) Gelatin nanoparticle fabrication and optimization of the particle size. Physica Status Solidi A: Applications and Materials Science, 205(12), 2898-2902.

Kang, S., Yasuda, M., Miyasaka, H., Hayashi, H., Kawasaki, M., Umeyama, T., Matano, Y., Yoshida, K., Isoda, S., Imahori, H. (2008) Light-Harvesting and Energy Transfer in Multiporphyrin-Modified CdSe Nanoparticles. ChemSusChem, 1(3), 254-261.

Karel, M. (1980) Lipid oxidation, secondary reactions, and water activity of foods. In: Autoxidation in Food and Biological System. Simic, M. G. and Karel, M. (Ed.), Plenum Press, London.

Katz, E. E. and Labuza, T. P. (1981) Effect of water activity on the sensory crispness and mechanical deformation of snack food products. J. Fd Sci., 46, 403-9.

Kerman, K., Saito, M., Tamiya, E. (2008) Electroactive chitosan nanoparticles for the detection of single-nucleotide polymorphisms using peptide nucleic acids. Analytical and Bioanalytical Chemistry, 391(8), 2759-2767.

Kommareddy, S., Amiji, M., (2005) Preparation and evaluation of thiol-modified gelatin nanoparticles for intracellular DNA delivery in response to glutathione. Bioconj. Chem. 16, 1423-1432.

Kondo, S., Hayashi, S. (1991) (Mitsubishi Heavy Industries, Ltd., Japan). Shape memory polymer for use as sensor in frozen preservation. Jpn. Kokai Tokkyo Koho, 7 pp.

Krasnowska,E., Gratton, E., Parasassi, T. (1998) Prodan as a membrane surface fluorescence probe: partitioning between water and phospholipid phases. Biophys. J. 74, 1984–1993.

Kreisman, L. N. and Labuza, T. P. (1978) Storage stability of intermediate moisture food process cheese food products. J. Fd Sci., 43, 341-4.

Labuza, T. P. (1975) Oxidative changes in foods at low and intermediate moisture levels In: Water activity: influences on food quality. Rockland, L. B. and Stewart, G. F. (Ed.), 605, Academic Press, New York

Labuza, T. P. and Saltmarch, M. (1981) Kinetics of browning and protein quality loss in whey powders under steady state and nonsteady state storage conditions. J. Fd Sci., 47, 92-6, 113.

Lee, H., Forte, J. (1980) A novel method for measurement of intravesicular pH using fluorescent probes. Biochim. Biophys. Acta, Biomembranes 601, 152-166.

Lian, W., Litherland, S., Badrane, H., Tan, W., Wu, D., Baker, H., Gulig, P., Lim, D., Jin, S. (2004) Ultrasensitive detection of biomolecules with fluorescent dye-doped nanoparticles. Analytical Biochemistry 334, 135-144.

Liang, S., Pierce, D., Amiot, C., Zhao, X. (2005) Photoactive nanomaterials for sensing trace analytes in biological samples. Synth. React. Inorg. Metal-Org. Nano-Metal Chem. 35, 661-668.

Litvinchuk, S., Sorde, N., Matile, S. (2005) Sugar sensing with synthetic multifunctional pores. J. Am. Chem. Soc. 127, 9316-9317.

Liu, J., Wang, F., Wang, L., Xiao, S., Tong, C., Tang, D., Liu, X. (2008) Preparation of fluorescence starch - nanoparticle and its application as plant transgenic vehicle. Journal of Central South University of Technology (English Edition), 15(6), 768-773.

Maali, A., Cardinal, T., Treguer-Delapierre, M. (2003) Intrinsic fluorescence from individual silver nanoparticles. Physica E: Low-Dimensional Systems & Nanostructures (Amsterdam, Netherlands), 17(1-4), 559-560.

Manso, J., Mena, M. L., Yanez-Sedeno, P., Pingarron, J. M. (2008) Bienzyme amperometric biosensor using gold nanoparticle-modified electrodes for the determination of inulin in foods. Analytical Biochemistry, 375(2), 345-353.

Massey, J. (1998) Effect of cholesteryl hemisuccinate on the interfacial properties of phosphatidylcholine bilayers. Biochim. Biophys. Acta 1415, 193–204.

Mills, A. (2005) Oxygen indicators and intelligent inks for packaged food. Chemical Society Reviews 34, 1003-1011.

Moorthy, J.N., Shevchenko, T., Magon, A., Bohne, C. (1998) Paper acidity estimation: Application of pH-dependent fluorescence probes. J Photochem. Photobiol. A: Chem. 113, 189-195

Morton, R.A. (1975) *Biochemical Spectroscopy, Volume 2.* Adam Hilger, London.

Murphy, C. (2002) Optical sensing with quantum dots. Anal. Chem. 74, 5210A-526A

O'Mahony, F., O'Riordan, T., Papkovskaia, N., Kerry, J., Papkovsky, D. (2005) Non-destructive assessment of oxygen levels in industrial modified atmosphere packaged cheddar cheese. Food Control 17, 286-292.

Oppenheim, R., Stewart, N. (1979) The manufacture and tumor cell uptake of nanoparticles labeled with fluorescein isothiocyanate. Drug Develop. Ind. Pharm. 5, 563-571.

Parasassi, T., De Stasio, G., d'Ubaldo, A., Gratton, E. (1990) Phase fluctuation in phospholipid membranes revealed by Laurdan fluorescence. Biophys. J. 57, 1179–1186.

Parasassi, T., Di Stefano, M., Loiero, M., Ravagnan, G., Gratton, E. (1994) Cholesterol modifies water concentration and dynamics in phospholipid bilayers: a fluorescence study using Laurdan probe. Biophys. J. 66, 763–768.

Park, J. H., Gu, L., von Maltzahn, G., Ruoslahti, E., Bhatia, S. N., Sailor, M. J. (2009) Biodegradable luminescent porous silicon nanoparticles for in vivo applications. Nature Materials, 8(4), 331-336.

Partington, J.R. (1961) *A History of Chemistry, Volume 2.* Macmillan & Co., Ltd., London.

Pastorino, A. J., Hansen, C. L., McMahon, D. J. (2003) Effect of pH on the chemical composition and structure-function relationships of Cheddar cheese. Journal of Dairy Science, 86(9), 2751-2760.

Petriella, C., Resnik, S. L., Lozano, R. D. and Chirife, J. (1985) Kinetics of deteriorative reactions in model food systems of high water activity: color changes due to nonenzymatic browning. J. Fd Sci., 50, 662-6.

Pravinata, L.C. & Ludescher, R.D. (2003) Molecular Mobility Studies of Amorphous Sucrose and Cornstarch using a Novel Technique, Luminescence Spectroscopy. IFT Annual Meeting, July 2003, Chicago, IL.

Quast, D. G. and Karel, M. (1972) Effects of environmental factors on the oxidation of potato chips. J. Fd Sci., 37, 584-8.

Ravindranath, S. P., Mauer, L. J., Deb-Roy, C., Irudayaraj, J. (2009) Biofunctionalized Magnetic Nanoparticle Integrated Mid-Infrared Pathogen Sensor for Food Matrixes. Analytical Chemistry, 81(8), 2840-2846.

Revilla, M., Tolivia, D., Tarrago, J. (1986) A new and permanent staining method for starch granules using fluorescence microscopy. Stain Technology 61, 151-154.

Sablani, S. S., Al-Belushi, K., Al-Marhubi, I., Al-Belushi, R. (2007) Evaluating stability of vitamin C in fortified formula using water activity and glass transition. International Journal of Food Properties, 10(1), 61-71.

Salgo, M., Cueto, R., Pryor, W. (1995) Effect of lipid products on liposomal membranes detected by laurdan fluorescence. Free Rad. Biol. & Med. 19, 609-616.

Seguchi, M. (1986) Dye binding to the surface of wheat starch granules. Cereal Chem. 64, 518-520.

Sheehan, J. J., Guinee, T. P. (2004) Effect of pH and calcium level on the biochemical, textural and functional properties of reduced-fat Mozzarella cheese. International Dairy Journal, 14(2), 161-172.

Shimada, T., Ookubo, K., Komuro, N., Shimizu, T., Uehara, N. (2007) Blue-to-Red Chromatic Sensor Composed of Gold Nanoparticles Conjugated with Thermoresponsive Copolymer for Thiol Sensing. Langmuir, 23(22), 11225-11232.

Shinohara, K., Sugil, Y., Okamoto, K., Madarame, H., Hibara, A., Tokeshi, M., Katamori, T. (2004) Measurement of pH field of chemically reacting flow in microfluidic devices by laser-induced fluorescence. Measurement Sci. & Tech. 15, 955-960.

Silbert, L., Ben Shlush, I., Israel, E., Porgador, A., Kolusheva, S., Jelinek, R. (2006) Rapid chromatic detection of bacteria by use of a new biomimetic polymer sensor. Applied and Environmental Microbiology, 72(11), 7339-7344.

Sjöback, R., Nygren, J., Kubista, M. (1995) Absorption and fluorescence properties of fluorescein. Spectrochimica Acta Part A 51, L7-L21.

Taylor, J., Fang, M., Nie, S. (2000) Probing specific sequences on single DNA molecules with bioconjugated fluorescent nanoparticles. Anal. Chem. 72, 1979-1986.

Troller, J. A. and Christian, J. H. B. (1978) Water Activity and Food, Academic Press, NY.

Volmar, Y. (1936) Acidimetry and alkalimetry in presence of some fluorescent indicators. Documentation Scientifique 5, 33-39.

Wang, L., Ling, D., Bian, G., Xia, T., Chen, H., Wang, L., Cao, Q., Li, L. (2004) Application of organic nanoparticles as fluorescence probe in the determination of nucleic acids. Anal. Letters 37,1811-1822.

Wang, L., Wang, L., Xia, T., Bian, G., Dong, L., Tang, Z., Wang, F. (2005) A highly sensitive assay for spectrofluorimetric determination of reduced glutathione using organic nano-probes. Spectrochim. Acta, Part A: Molec. Biomolec. Spectro. 61A, 2533-2538.

Wang, X-H., Li, F., Liu, J-F., Pope, M. T. (2004), Preparation of a New Polyoxometalate-based Nanoparticles. Chinese Chemical Letters Vol. 15, No. 6, pp 714-716.

Wolfbeis, O. S. (1985) Molecular Luminescence Spectroscopy: Methods & Applications, Volume 1, Chapter 3.

Wolfbeis, O. S., Fürlinger, E., Wintersteiger, R. (1982) Solvent- and pH-Dependence of the Absorption and Fluorescence Spectra of Harman: Detection of Three Ground State and Four Excited State Species. Monatshefte für Chemic 113, 509-517.

Wolfbeis, O. S., Fürlinger, E. (1982) The pH-Dependence of the Absorption and Fluorescence Spectra of Harmine and Harmol: Drastic Differences in the Tautomeric Equilibria of Ground and First Excited Singlet State. Zeitschrift für physikalische chemie Neue Folge Bd. 129, S. 171-183.

Yguerabide, J., Talavera, E., Alvarez, J. M., Quintero, B. (1994) Steady-state fluorescence method for evaluating excited state proton reactions: application to fluorescein. Photochem. Photobiol. 60, pp. 435–441.

Zhang, Z., Xu, K., Xing, Z., Zhang, X. (2005) A nanosized Y2O3-based catalytic chemiluminescent sensor for trimethyl amine. Talanta 65, 913-917.

Zhai, F., Li, D., Zhang, C., Wang, X., Li, R. (2008) Synthesis and characterization of polyoxometalates loaded starch nanocomplex and its antitumoral activity. European Journal of Medicinal Chemistry, 43(9), 1911-1917.

Zheng, A., Wang, K., Hao, R., Li, M., Wang, J., Zhang, Q. (2007) Preparation, release in vitro and biological activity of thymopentin-loaded pH-sensitive chitosan nanoparticles for oral administration. Zhongguo Yaoxue Zazhi, 42(9), 679-685.

Chapter 2: Materials and Methods

Materials

Gelatin type A (100 Bloom) was from Vyse Gelatin Company (Schiller Park, IL). Glutaraldehyde solution grade I (25% in H_2O), fluorescein 5(6)-isothiocyanate (FITC) for fluorescence ≥ 90% (HPLC), soluble starch from potato, toluene, chloroform, sodium phosphate dibasic heptahydrate, sodium phosphate monobasic anhydrous, sodium acetic trihydrate, potassium sulfate, Span-80, Trizma® base, phosphoryl chloride, harmane and quinine hemisulfate monohydrate were purchased from Sigma-Aldrich. Phosphoric acid (85%), hydrochloride acid, acetic acid glacial, acetone and ethanol were obtained from Fisher Scientific. Milli-Q water (18.3 MΩ) was used in all experiments.

Methods

Preparing starch nanoparticles

Starch nanoparticles were prepared by a W/O nanoemulsion method using phosphoryl chloride as a cross-linker (Wang et al., 2004). 0.5 g of soluble starch was added to 5 ml distilled water and then heated in a boiling water-bath until the mixture turned transparent to form an aqueous starch solution. This aqueous solution was cooled to room temperature and 100 mg of K_2SO_4 was added. This aqueous phase was added drop-wise to an oil-phase (containing 100 mL of $C_6H_5CH_3$, 100 mL of $CHCl_3$ and 4 mL of surfactant Span-80) with stirring. It was kept stirring until a microemulsion was formed which was then treated by Sonifier cell disruptor W185 from Heat Systems-Ultrasonics Inc (Farmingdale, NY), for 5 min in order to obtain nanoemulsion. To this nanoemulsion, 600 µL of $POCl_3$ was added

and stirring was continued for another 1 h. The nanoemulsion was washed with acetone and then ethanol three times, respectively, to obtain white solid starch nanoparticles. The solid was first dissolved in distilled water and passed through 0.2 μm Whatman® PES filter to remove any particle with diameter larger than 200 nm. Then dissolved nanoparticles were dialyzed against 1.5L distilled water for 2 days and further freeze-dried to obtain the dry powder. Dry powder of starch nanoparticles was kept in a refrigerator.

In the original method, polyoxometalates, instead of K_2SO_4, were added and encapsulated in starch nanoparticles. However, with removal of polyoxometalates, there were no white solid starch nanoparticles precipitated upon washing nanoemulsion with acetone and ethanol. Hence, K_2SO_4 was added as a substitute for polyoxometalates. Other salts may also work but have not been tried.

Washing nanoemulsion with acetone and ethanol is important for two reasons. First, it precipitates the nanoparticles from W/O emulsion. Second, it helps remove remaining phosphoryl chloride and dilute the acidity of the nanoparticles solution, which comes from the reaction of phosphoryl chloride with water. Solid starch nanoparticles can easily turn dark when dissolved in water if not well washed by acetone and ethanol. High acidity of nanoparticles solution may be a potential reason.

The dialysis before freeze-drying aims to further dispose of phosphoryl chloride and other impurities like potassium sulfate. Removing the unreacted phosphoryl chloride can minimize over-crosslinking of nanoparticles, which would decrease the dissolvability of

starch nanoparticles in water during the storage. The dry powder of starch nanoparticles then can be stored in refrigerator for a couple of months.

Preparing gelatin nanoparticles

Preparation of gelatin nanoparticles was based on a two-step desolvation method (Azarmi et al., 2006). 1.25 g gelatin was dissolved in 25 mL distilled water under stirring and constant heating. 25 mL acetone was added to the gelatin solution as a desolvating agent to precipitate the high molecular weight (HMW) gelatin. After two hours, the supernatant was discarded and the HMW gelatin was re-dissolved by adding 25 mL distilled water under stirring and constant heating. The pH of the gelatin solution was adjusted to about 2.5. 75 mL acetone was added drop-wise to form nanoparticles. One hour later, 250 μL of 25% glutaraldehyde solution was used as a cross-linking agent for preparing nanoparticles. The solution was stirred for 12 h after cross-linking. Remaining acetone was evaporated and the resultant nanoparticles were dialyzed against 1.5 L distilled water for 2 days. Water was changed twice every day. Dialyzed gelatin nanoparticles solution was further freeze-dried to obtain the dry powder. Dry powder of gelatin nanoparticles was kept in a refrigerator.

The dialysis step in the process of making gelatin nanoparticles plays the same role as it does in making starch nanoparticles, helping remove extra cross-linking agent (glutaradehyde). Otherwise, the solubility of gelatin nanoparticles decreases during storage.

Determining starch or gelatin nanoparticles' size

Diluted starch nanoparticle solution and gelatin nanoparticle solution were tested using a 90Plus Particle Size Analyzer from Brookhaven Instruments Corporation (Holtsville, NY) before labeling to determine particle sizes. The dimensions of both starch and gelatin nanoparticles varied in different batches. However, most starch nanoparticles were within the range of 100-200 nm, while gelatin nanoparticles varied from 30-50 nm.

Labeling starch and gelatin nanoparticles

To label starch nanoparticles, 100 mg dry powder of starch nanoparticles was dissolved in 5 mL 0.2 mM quinine or harmane solution and soaked for 3-4 hours. Then the solution was dialyzed against 1.5 L distilled water for 3 days. Water was changed twice every day.

To label gelatin nanoparticles, 100 mg dry powder of gelatin nanoparticles was dissolved in 5 mL distilled water. 10mg/mL stock solution of FITC was prepared in advance and 38.9 μL stock solution was added to the gelatin nanoparticle solution. The solution was kept and stirred at room temperature for 3-4 hours. After that the solution was dialyzed against 1.5 L distilled water for 3 days. Water was changed twice every day.

If we assume all probes would be attached onto nanoparticles, the final concentration of probes when conducting fluorescent tests would be 1×10^{-5} M. However, quinine or harmane can only be non-covalently attached onto starch nanoparticles, so the actual probe concentration when conducting fluorescent tests would be much lower. Although FITC can spontaneously react with amine ($-NH_2$) and sulfhydryl (-SH) groups on gelatin, not all

FITC would be covalently attached onto gelatin as well. In this research, about 50% FITC was covalently labeled onto gelatin nanoparticles. Hence, the final concentration of labeled FITC when conducting tests would be 5×10^{-6} M, while the final concentration of gelatin nanoparticles was 1 mg/ml. The molecular weight of amino acid residue of gelatin is about 93 g/mol on average (based on previous research in the lab). Therefore, the molar concentration of amino residue in gelatin nanoparticles solution was 0.0107 M ($1/93\approx 0.0107$); the ratio of FITC probe to amino residue was about 1:2,150 (5×10^{-6}: 0.0107) on average.

The dialysis during the labeling process aims to remove unlabeled free probes. Detectable fluorescent signals of free probes were observed normally in the first two batches of dialysate and almost disappeared or became hard to detect after two days of dialyzing, so three days dialyzing can ensure the removal of free probes.

Preparing pH buffer solutions

Buffer solutions with pH around 2.5, 3.0 and 3.5 were prepared with Na_2PO_4/H_3PO_4; solutions with pH around 4.0, 4.5 and 5.0 were prepared with CH_3COOH/CH_3COONa; solutions with pH around 5.5, 6.0, 6.5, 7.0 and 7.5 were prepared with NaH_2PO_4/Na_2HPO_4; and solutions with pH around 8.0, 8.5 and 9.0 were prepared with Trizma® base and HCl. All pH's were determined by AR15 pH meter at room temperature. Buffer solutions were stored at room temperature.

Preparing food samples

Several food products were purchased from a supermarket and used in this research to test pH nanoparticle sensors; these included Sprite, Orangeade Snapple, Snapple iced tea, Goya® papaya nectar, Hero® guava nectar, Rienzi® pear nectar, several Stop&Shop® canned foods, Tuscan® fat free milk, Kuang®soymilk, Knorr®chicken soup, Stop&Shop® mayonnaise, DANNON® yogurt, Turkey Hill® green tea, Lipton® green tea, Wei-chuan® soy sauce, Tiger Tiger® fish sauce, Marukan® Rice vinegar, Shoprite®grape juice, Bolthouse farms® carrot juice, Wei-chuan® aloe juice, homemade watermelon juice and homemade mayonnaise. Homemade water melon juice was extracted from fresh water melon. Homemade mayonnaise was made using a blender and base on this recipe: 180 ml Guaranteed Value™ Vegetable oil, 20 ml rice vinegar and 1 egg yolk. All clear liquids, yogurt, Stop&Shop® mayonnaise and homemade mayonnaise were directly used in fluorescent tests and tested by pH meter to obtain the food pH. The liquids of all canned foods were used to conduct fluorescent tests and tested by pH meter to obtain the pH of canned foods. All fruit nectars and turbid fruit juices were vacuum filtered first with No. 2 filter paper (8 μm) from Whatman to remove most fruit fibers, the filtrates then were used in fluorescent tests and pH of the filtrates was taken on pH meter to be used as the food pH. All food samples' pH's were determined on the same day that fluorescent tests were performed. The food sample's pH may vary if the pH's were not obtained on the same day.

Methodology

The pH-dependence of probe fluorescence depends upon changes in its molar absorptivity with pH (Morton, 1975). Hence, for the probes used in this research, the fluorescence intensity $I(pH,\lambda_{ex})$ as a function of pH and excitation wavelength is (Shinohara et al., 2004):

$$I(pH, \lambda_{ex}) = I_o(\lambda_{ex})\ \Phi\ \varepsilon(pH, \lambda_{ex})\ C\ F$$

Where $I_o(\lambda_{ex})$ is the light intensity as a function of excitation wavelength; Φ is the probe quantum yield; $\varepsilon(pH, \lambda_{ex})$ is the pH- and wavelength-dependent probe molar absorptivity; C is the molar concentration of probe and F is the detection efficiency of the instrument at the specific emission wavelength. For fixed λ_{ex1} and λ_{ex2}, the ratio:

$$I_{\lambda ex1}/I_{\lambda ex2}(pH) = \kappa\ \varepsilon(pH, \lambda_{ex1}) / \varepsilon(pH, \lambda_{ex2})$$

As Φ, C and F all are canceled out. $\kappa = I_o(\lambda_{ex1}) / I_o(\lambda_{ex2})$ is a constant at fixed λ_{ex1} and λ_{ex2}. Hence, the ratio of $I_{\lambda ex1}/I_{\lambda ex2}$ (pH) is a pH-dependent function, which was employed in this research to indicate pH.

Quinine absorption has an exact isosbestic point at 295 nm; the ratio of fluorescent intensities collected at λ_{ex1} = 345 nm and λ_{ex2} = 295 nm corresponds to the maximum change in ε (Morton, 1975). Harmane absorption also has an isosbestic point at λ_{ex1} = 350 nm; the other λ_{ex2} was selected at 300 nm to reach the maximum change in ε (Wolfbeis et al., 1982). FITC is a derivative of fluorescein. Based on fluorescein absorption property and our trials, λ_{ex1} = 435nm and λ_{ex2} = 460nm were selected for exciting FITC (Moorthy et al., 1998; Sjöback et al., 1995).

Fluorescent measurements of starch or gelatin nanoparticle sensors in buffer solutions

150 μL labeled starch or gelatin nanoparticle sensor solution and 2850 μL buffer solution were mixed in a cuvette and tested by Cary Eclipse fluorescence spectrophotometer from Varian Inc. (Palo Alto, CA). The final concentration of starch or gelatin nanoparticles was ~1 mg/mL. 150 μL 0.2mM corresponding probe solution and 2850 μL buffer solution were mixed in another cuvette to be tested as comparison. The final concentration of probe solution was 1×10^{-5} M. All measurements were done at room temperature.

Fluorescent measurements of labeled nanoparticle sensors in food samples

For all food samples except mayonnaise and yogurt, 150 μL labeled nanoparticle sensor solution and 2850 μL prepared food sample were mixed in a cuvette to be tested. 150 μL water and 2850 μL prepared food sample were mixed in another cuvette to be tested as background. The final concentration of nanoparticles was ~1 mg/mL.

For mayonnaise, only FITC-labeled gelatin nanoparticle (FGNP) sensors were tested. 100 μL of 60 mg/mL FGNP sensor solution was added into 3.0 g mayonnaise making the gelatin nanoparticles 0.2% (w/w) in mayonnaise. After simply stirring to disperse nanoparticles, the sample was tested by fiber optic coupler attached to Cary Eclipse fluorescence spectrophotometer. Mayonnaise with added 0.2% (w/w) water was tested as the background. Yogurt sample was tested in the same way.

Data analysis

All data were analyzed using Igor (WaveMetrics Inc., Lake Oswego, OR). Areas of emission spectra were integrated before fitting while peak intensities were obtained by fitting emission spectra using either log-normal functions or a sum of two log-normal functions (Maroncelli, 1987). The ratios of peak intensities and peak areas at two different excitation wavelengths were used to develop calibration curves.

References

Azarmi, S., Huang, Y., Chen, H., McQuarrie, S., Abrams, D., Roa, W., Finlay, W. H., Miller, G. G., Löbenberg, R. (2006) Optimization of a two-step desolvation method for preparing gelatin nanoparticles and cell uptake studies in 143B osteosarcoma cancer cells. J Pharm Pharmaceut Sci 9(1):124-132.

Moorthy, J.N., Shevchenko, T., Magon, A., Bohne, C. (1998) Paper acidity estimation: Application of pH-dependent fluorescence probes. J Photochem. Photobiol. A: Chem. 113, 189-195

Morton, R.A. (1975) *Biochemical Spectroscopy, Volume 2.* Adam Hilger, London.

Sjöback, R., Nygren, J., Kubista, M. (1995) Absorption and fluorescence properties of fluorescein. Spectrochimica Acta Part A 51, L7-L21.

Shinohara, K., Sugil, Y., Okamoto, K., Madarame, H., Hibara, A., Tokeshi, M., Katamori, T. (2004) Measurement of pH field of chemically reacting flow in microfluidic devices by laser-induced fluorescence. Measurement Sci. & Tech. 15, 955-960.

Wang, X-H., Li, F., Liu, J-F., Pope, M. T. (2004), Preparation of a New Polyoxometalate-based Nanoparticles. Chinese Chemical Letters Vol. 15, No. 6, pp 714-716.

Wolfbeis, O. S., Fürlinger, E., Wintersteiger, R. (1982) Solvent- and pH-Dependence of the Absorption and Fluorescence Spectra of Harman: Detection of Three Ground State and Four Excited State Species. Monatshefte für Chemic 113, 509-517.

Maroncelli, M., Fleming, G. R. (1987) Picosecond solvation dynamics of coumarin 153: the importance of molecular aspects of salvation, J. Chem. Phys. 86, 6221 – 6239.

Chapter 3: Characterizing quinine labeled starch nanoparticle (QSNP) sensors

Results

QSNP sensors fluorescence tests in various pH buffers

In Fig. 1 and Fig. 2 are shown the emission spectra of quinine-labeled starch nanoparticle (QSNP) sensors in buffer solutions of pH from 3.0 to 5.0. Emission maxima of QSNP with excitation at 345 nm blue shifted from around 452 nm to around 392 nm as the pH increased from 3.0 to 5.0. Emission maxima of QSNP with excitation at 295 nm blue shifted from around 452 nm to around 387 nm as the pH increased from 3.0 to 5.0. Emission spectra of quinine in buffer solutions at the same pH exhibit the same behavior (Moorthy, 1998).

The ratio of peak intensity of quinine solution (1×10^{-5} M) and QSNP sensors (~1 mg/ml) were determined in buffer solutions at pH 2.5 - 7.5. Both solutions showed almost the same fluorescent behavior. In Fig. 3 is shown that the peak intensity decreases as the pH increases. From pH 2.5 to 3.5, the peak intensity ratio has very small change. However, from pH 4.0 to 5.0, there is a sharp decrease in peak intensity ratio from around 2.5 to 1.0. The peak intensity ratio finally reaches a plateau when pH is above 5.0. The peak area ratio against pH is also showed in Fig. 4, which displays similar behavior to the changes of peak intensity ratio.

Fluorescent tests of QSNP sensors in various food samples

QSNP sensors were applied to test food pH in Snapple, Sprite, green tea and guava nectar. The fluorescent intensity of QSNP excited at 345 nm in each food sample seemed to be appropriate for the concentration used. However, the fluorescent intensity of QSNP sensors excited at 295 nm in each food sample was much lower than expected, making the peak intensity ratio much higher compared to peak intensity ratio of quinine solution at the same pH condition. The example of applying QSNP sensors to test pH in Snapple is graphed in Fig. 5 and Fig. 6.

Discussion

Quinine was non-covalently bonded to starch nanoparticles. Comparisons of quinine and QSNP sensors in buffer solutions of various pH's demonstrate that quinine bound starch naoparticles retained the same fluorescent character as free quinine.

The emission spectra of quinine are reported as a combination of two emission spectra corresponding to that of dicationic (ca. 440 nm) and monocationic (ca. 385 nm) species as shown in Fig. 7 (Schulman et al., 1974). The pKa value of aromatic heterocyclic nitrogen is reported to be 4.9 (Moorthy et al., 1998). Other references also report this pKa value as 4.30 (Schulman et al., 1974) and 5.07 (Merck Index 14th, 2006). Despite the different pKa reported values, there is no doubt that when the pH changes from below 3.0 to above 5.0, the quinine molecules change from dications to monocations. The emission maxima shifts in this study also strongly supported that both quinine and QSNP sensors undergo this deprotonation procedure when pH changes from below 3.0 to above 5.0. Hence, this

deprotonation is the reason for the blue shifts of quinine and QSNP sensors. This deprotonation is also the cause of the decreasing peak intensity ratio or area ratio of quinine and QSNP sensors when pH increases from 3.0 to 5.0. The existence of plateaus of intensity ratio or area ratio above pH 5.0 is evidence for one species of quinine molecule existing in solution.

The pKa value of aliphatic heterocyclic nitrogen is reported to be 9.7 (Merck Index 14^{th}, 2006). Hence, the aliphatic heterocyclic nitrogen is sufficiently basic to always remain protonated over the pH range from 2.5 to 7.5.

The performance of QSNP sensors in food samples was not good. For example, as shown in Fig. 5 and Fig. 6, the relative intensity of QSNP sensors in Snapple excited at λ_{ex} = 345 nm was about 26.5, while the relative intensity of QSNP sensors in Snapple excited at λ_{ex} = 295 nm was only 2.5, making the peak intensity ratio about 10, as much as 4 times more than expected ratio value (Snapple's pH is around 3.4 with the expected intensity ratio to be around 2.5). A possible complication is protein intrinsic fluorescence which is always excited at λ_{ex} = 280 nm or at λ_{ex} = 295 nm (Sherwin, 1971). However, in all food sample tests, the same amount of distilled water was added into the food sample and tested as background. When the fluorescence signal of QSNP sensors in food sample was corrected for the background, the effect of protein intrinsic fluorescence should be eliminated or at least minimized. We also tried to use λ_{ex1} = 345 nm and λ_{ex2} = 315 nm. QSNP sensors showed similar behavior as when excited at λ_{ex1} = 345 nm and λ_{ex2} = 295 nm. But the peak intensity ratio of Snapple was 2.48, about twice the expected peak intensity ratio, which is

1.26. Sprite was also tested at λ_{ex1} = 345 nm and λ_{ex2} = 315 nm. With the simplest ingredients, Sprite's peak intensity ratio was tested as 1.34. Comparing to the expect peak intensity ratio of 1.26, it was the best result we ever had.

Conclusion

Quinine could be non-covalently labeled onto starch nanoparticles. Detectable signal can be obtained even after three days dialysis in distilled water. QSNP sensors display emission maxima that blue shift in various pH buffer solutions as pH increases from 3.0 to 5.0; their peak intensity or peak area ratio with excitation of 345 and 295 nm also decreases. Beyond this range, QSNP sensors do not exhibit any apparent emission maxima shifts or peak intensity (area) ratio changes. Those features imply that QSNP sensors may be a good pH indicator in the pH range from 3.0 to 5.0. The application of QSNP sensors in food samples, however, was not successful. Although λ_{ex1} = 345 nm and λ_{ex2} = 315 nm were tried as well, QSNP sensors still performed not as expected. Further research should be investigated to clarify the behavior of QSNP sensors in food samples.

Besides quinine, harmane (Wolfbeis, 1982), fluorescein and pyranine (Moorthy, 1998) were also tried to be labeled onto starch nanoparticles. However, the last two probes did not give detectable fluorescence signal after three days dialysis against distilled water, which made QSNP and HSNP the only two starch nanoparticles based pH sensors so far.

Tables & Figures

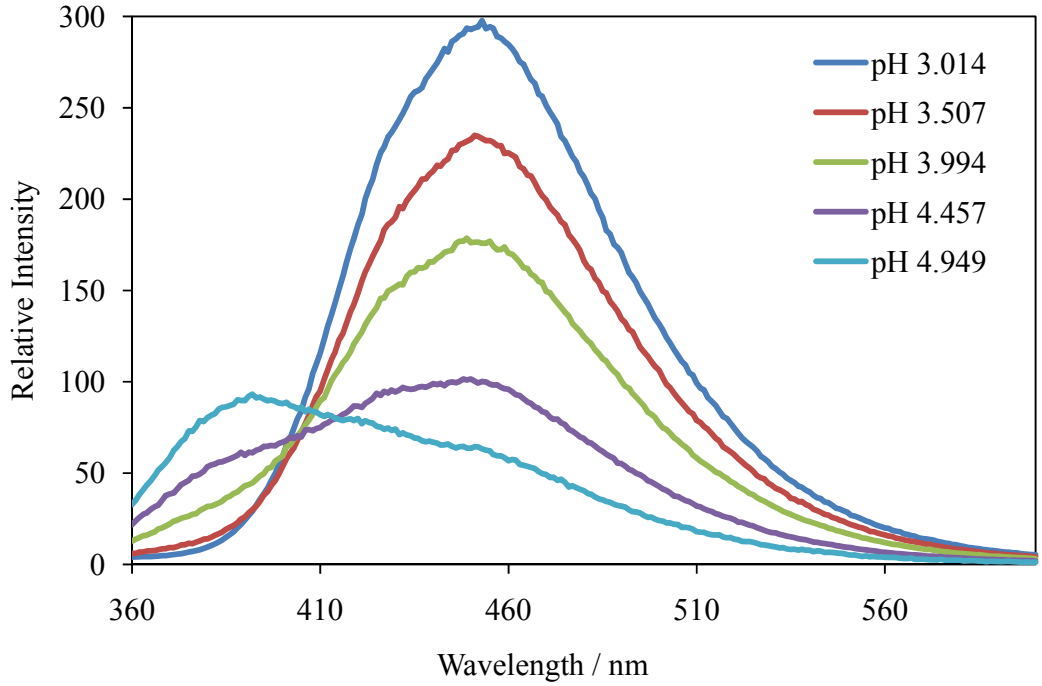

Figure 1: Emission spectra of QSNP sensors excited at λ_{ex} = 345 nm in various pH buffer solutions from pH 3.0 to 5.0.

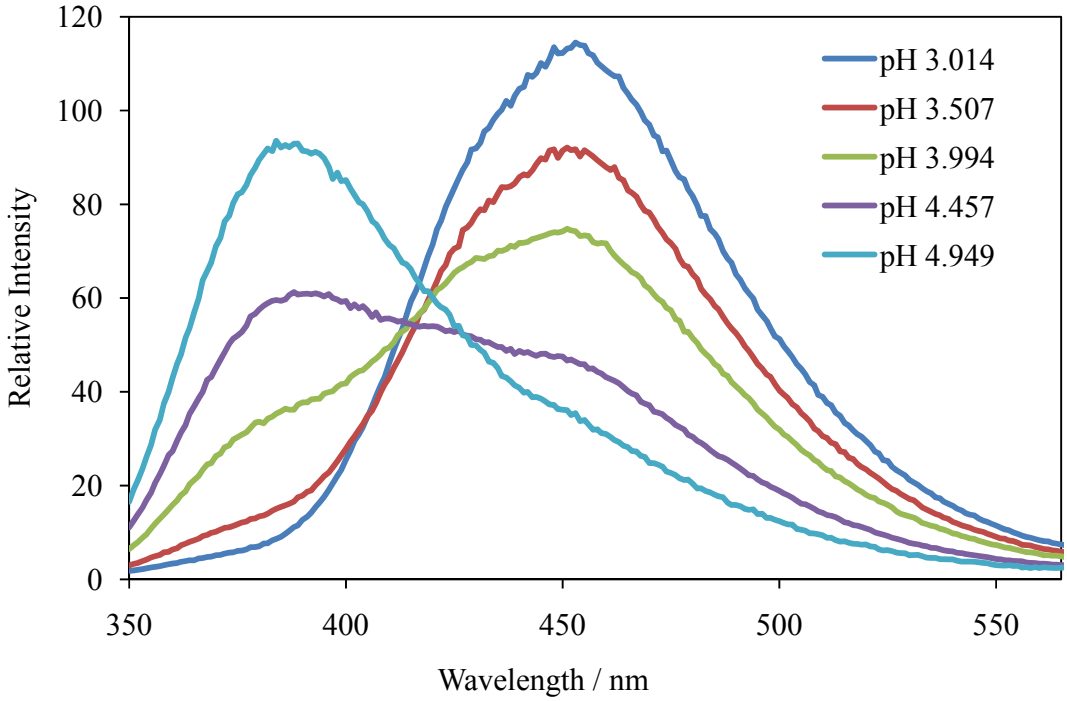

Figure 2: Emission spectra of QSNP sensors excited at λ_{ex} = 295 nm in various pH buffer solutions from pH 3.0 to 5.0.

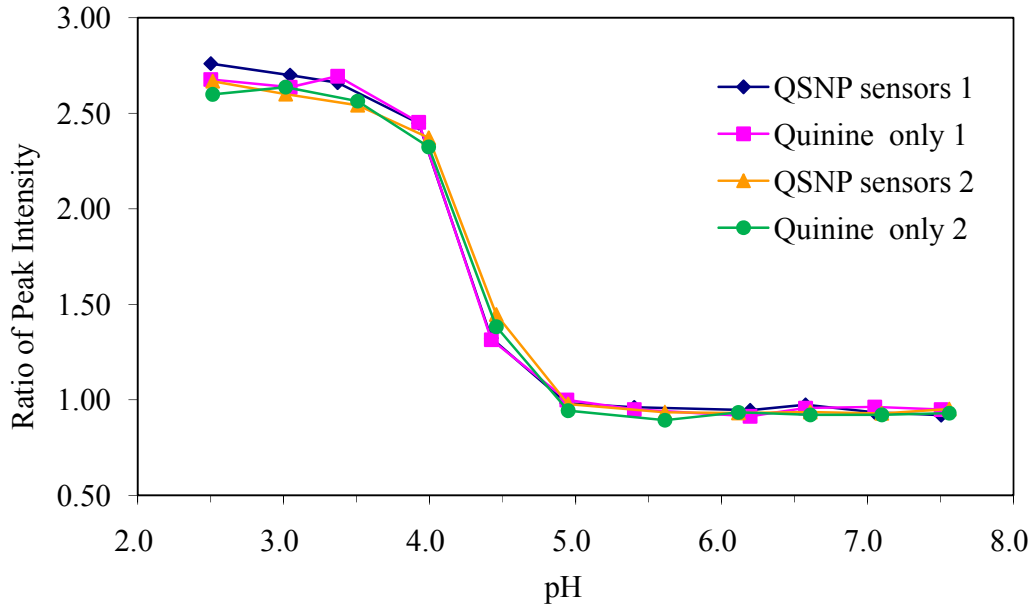

Figure 3: Comparison plot depicting the ratio of peak intensities $I_{345/295}$ of QSNP sensor and quinine solutions at various pH from 2.5 to 7.5. The number 1 and 2 indicate two batches of QSNP sensor and quinine solutions were made and tested in two different series of pH buffers.

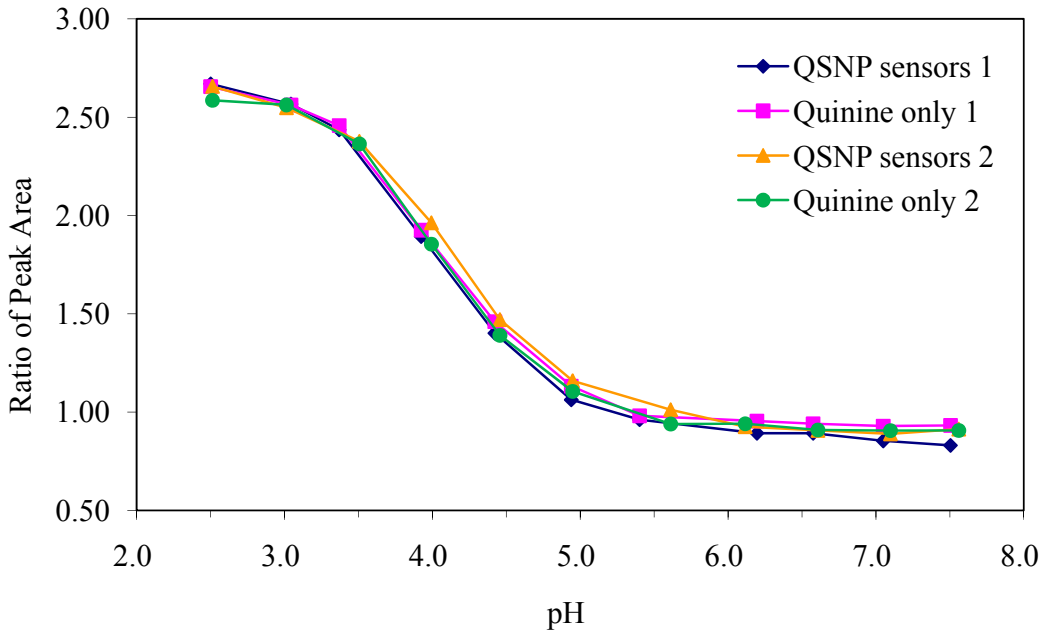

Figure 4: Comparison plot depicting the ratio of peak areas $A_{345/295}$ of QSNP sensor against quinine solutions at various pH from 2.5 to 7.5. The number 1 and 2 indicate two batches of QSNP sensor and quinine solutions were made and tested in two different series of pH buffers.

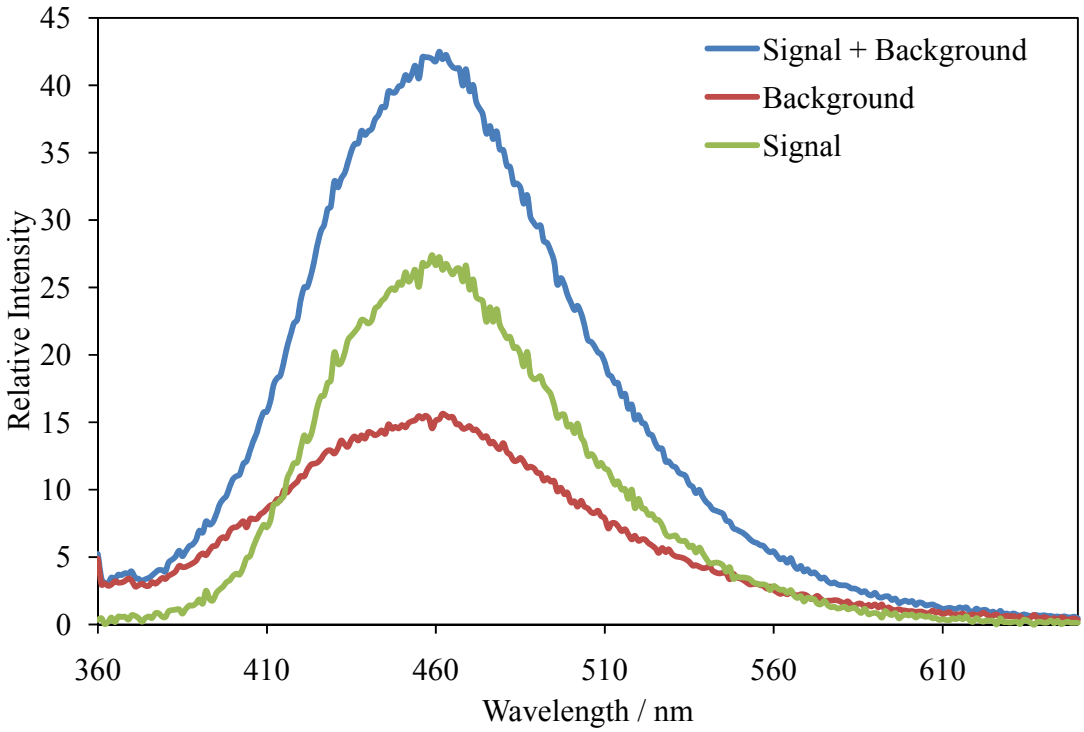

Figure 5: Fluorescence tests of QSNP sensors in Snapple, excited at λ_{ex} = 345 nm. Blue line is fluorescence signal of QSNP sensors in Snapple + Snapple background. Red line is only Snapple background. Green line = Blue line − Red line is the fluorescence signal of QSNP sensors in Snapple.

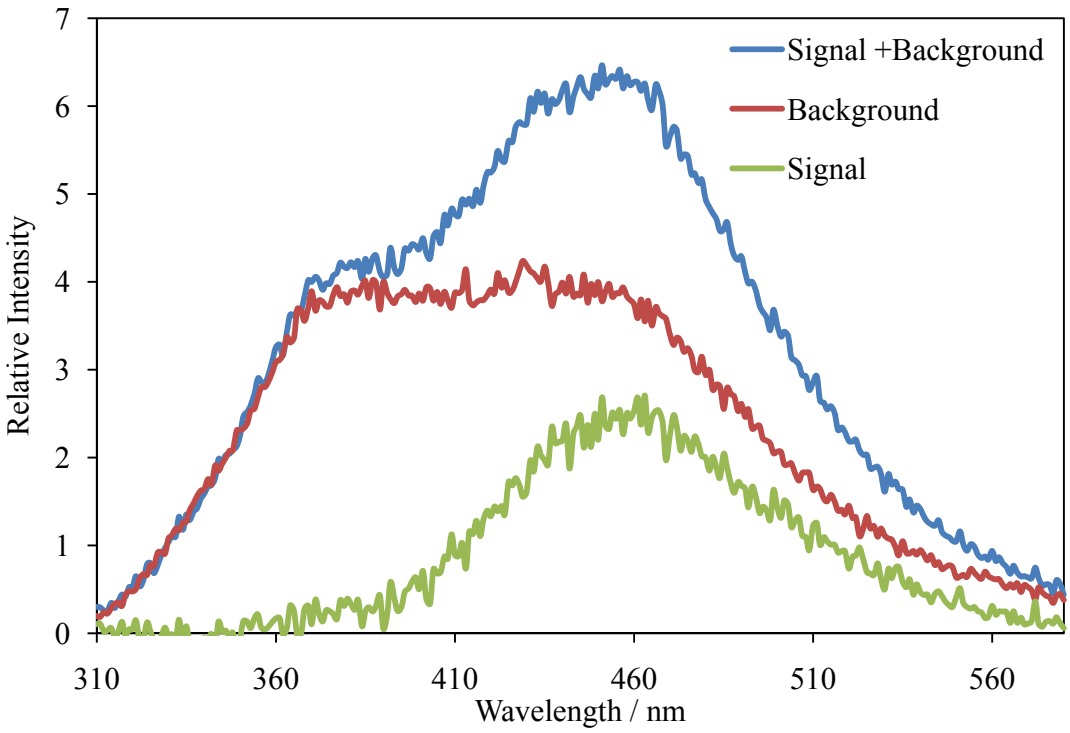

Figure 6: Fluorescence tests of QSNP sensors in Snapple, excited at λ_{ex} = 295 nm. Blue line is fluorescence signal of QSNP sensors in Snapple + Snapple background. Red line is only Snapple background. Green line = Blue line − Red line is the fluorescence signal of QSNP sensors in Snapple.

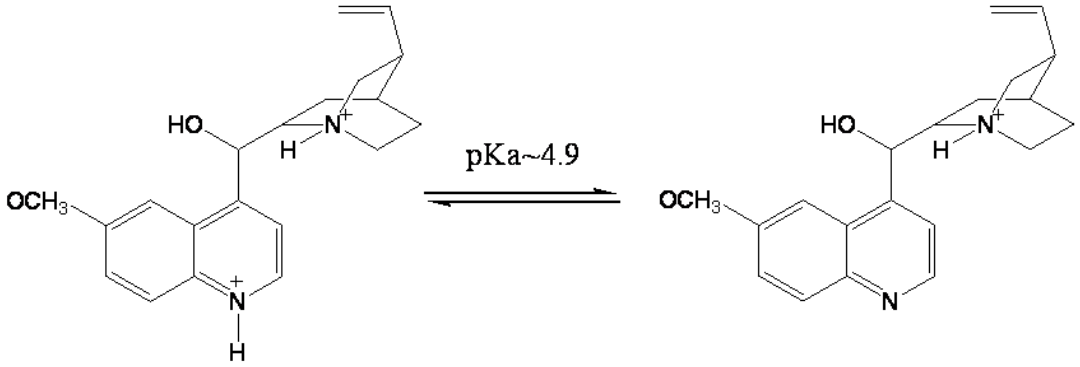

Figure 7: Dicationic (ca. 440 nm) and monocationic (ca. 385 nm) species of quinine (Schulman et al., 1974). The pKa value of aromatic heterocyclic nitrogen is reported to be 4.9 (Moorthy et al., 1998). Other references report this pKa value as 4.30 (Schulman et al., 1974) and 5.07 (Merck Index 14th, 2006).

References

Moorthy, J.N., Shevchenko, T., Magon, A., Bohne, C. (1998) Paper acidity estimation: Application of pH-dependent fluorescence probes. J Photochem. Photobiol. A: Chem. 113, 189-195

Schulman, S.G., Threatte, R.M., Capomacchia, A.C., Paul, W.A. (1974) Fluorescence of 6-methoxyquinoline, quinine, and quinidine in aqueous media. J. Pharm. Sci. 63, 876.

Sherwin S. L (1971) Solute Perturbation of Protein Fluorescence. The Quenching of the Tryptophyl Fluorescence of Model Compounds and of Lysozyme by Iodide Ion. Biochemistry, 10, 17, 3254-3263

Merck. (2006) Merck Index, 14th Edition.

Chapter 4: Characterizing harmane labeled starch nanoparticle (HSNP) sensors

Results

HSNP sensors fluorescent tests in various pH buffers

In Fig. 8 and Fig. 9 are shown fluorescent tests results of HSNP sensors in various pH buffer solutions from 5.5 to 9.0. Both harmane solution (1×10^{-5} M) and HSNP sensors showed almost the same peak intensity or peak area ratio in the same pH condition. The peak intensity or peak area ratio stayed almost unchanged at pH below 6.5 and increased very quickly as pH increased from 7.0 to 9.0. Meanwhile, harmane and HSNP sensors' emission spectra in buffer solutions exhibited the same behavior and did not display any shift when pH changed. Emission spectra of HSNP sensors are shown in Fig. 10 and Fig. 11. No food sample tests were conducted using HSNP sensors.

Discussion

Harmane, like quinine, has cationic and neutral species with emission maxima at around 430 nm and 381 nm, respectively (Wolfbeis et al., 1982). However, harmane did not exhibit out perceptible emission spectra shifts as quinine did when pH changed. The emission maxima of both harmane and HSNP sensors were around 430 nm, which corresponds to cationic species of harmane. The pKa value of aromatic heterocyclic nitrogen was reported as 7.37 and the neutral species was reported to be present in the pH range of 8~13 (Wolfbeis et al., 1982). However, the fluorescence intensity of the neutral species is rather weak based on previous research (Wolfbeis et al., 1982); no neutral species' emission was observed even at pH 9.0 in this study.

Both harmane's and HSNP sensors' peak intensity or peak area ratio increased as the pH increased from pH 7.0 to 9.0, which means harmane non-covalently bonded to starch nanoparticles has the same fluorescent behavior as free harmane. The continuously increasing ratio also indicates that HSNP sensors may be a potential food sensor working in basic environment.

Conclusion

Harmane could be non-covalently labeled onto starch nanoparticles to develop HSNP sensors. Detectable signal of HSNP sensors can be obtained after three days dialysis against distill water. HSNP sensors do not exhibit emission maxima shift in the pH range of 5.5~9.0. When pH is below 7.0, the peak intensity or peak area ratio of HSNP sensors is constant. However, the peak intensity or peak area ratio continuously increases with pH from 7.0 to 9.0, which implies that HSNP sensors can only be applied in weak basic conditions.

Tables & Figures

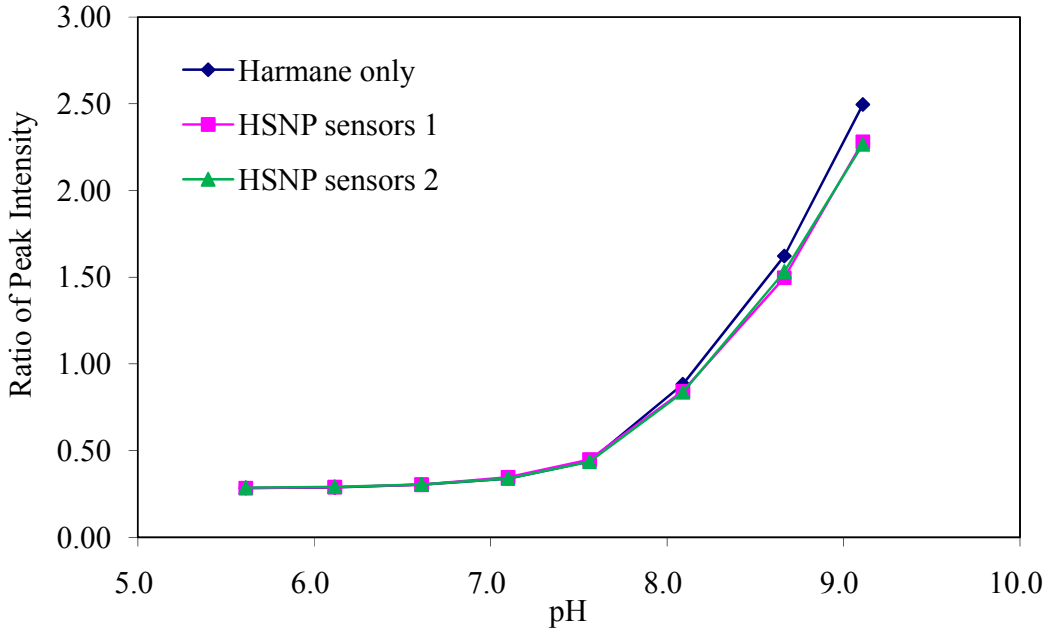

Figure 8: Plot of the ratio of peak intensities, $I_{350/300}$, of HSNP sensor (HSNP sensors 1 and HSNP sensors 2 are two batches of HSNP) and harmane solutions at various pH's.

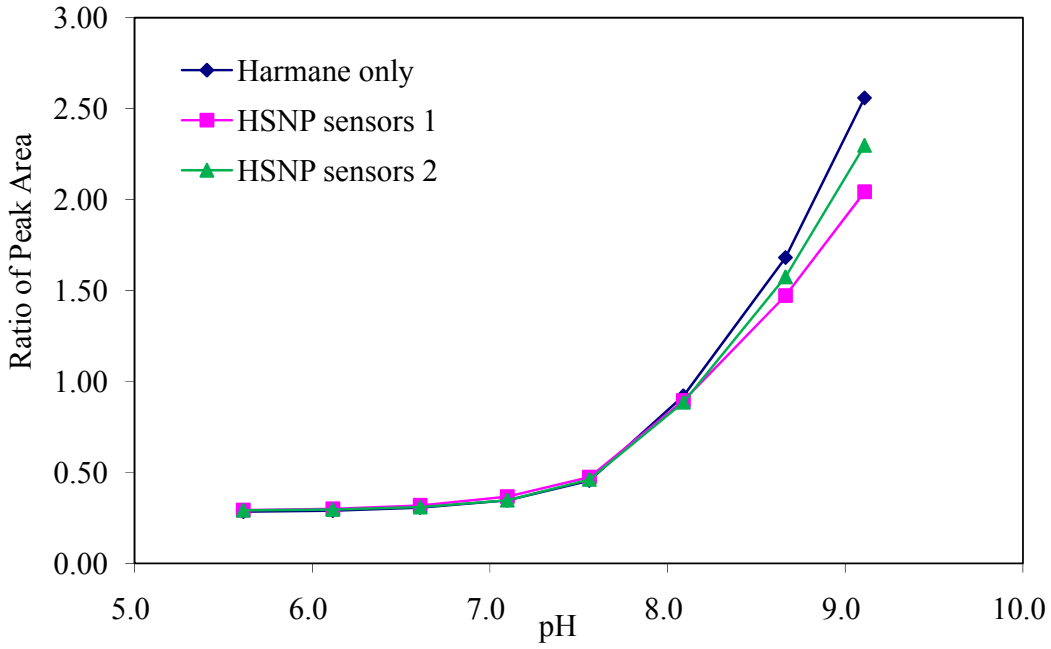

Figure 9: Plot of the ratio of peak areas, $A_{350/300}$, of HSNP sensor (HSNP sensors 1 and HSNP sensors 2 are two batches of HSNP) and harmane solutions at various pH's.

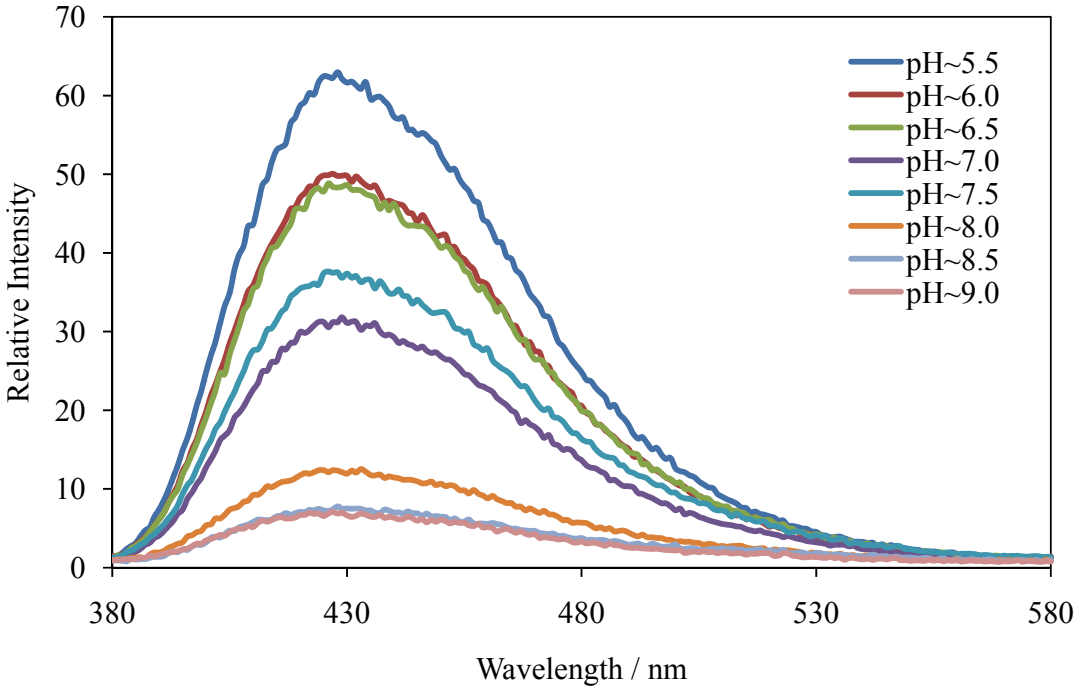

Figure 10: Emission spectra of HSNP sensors excited at λ_{ex} = 300 nm in various pH buffer solutions.

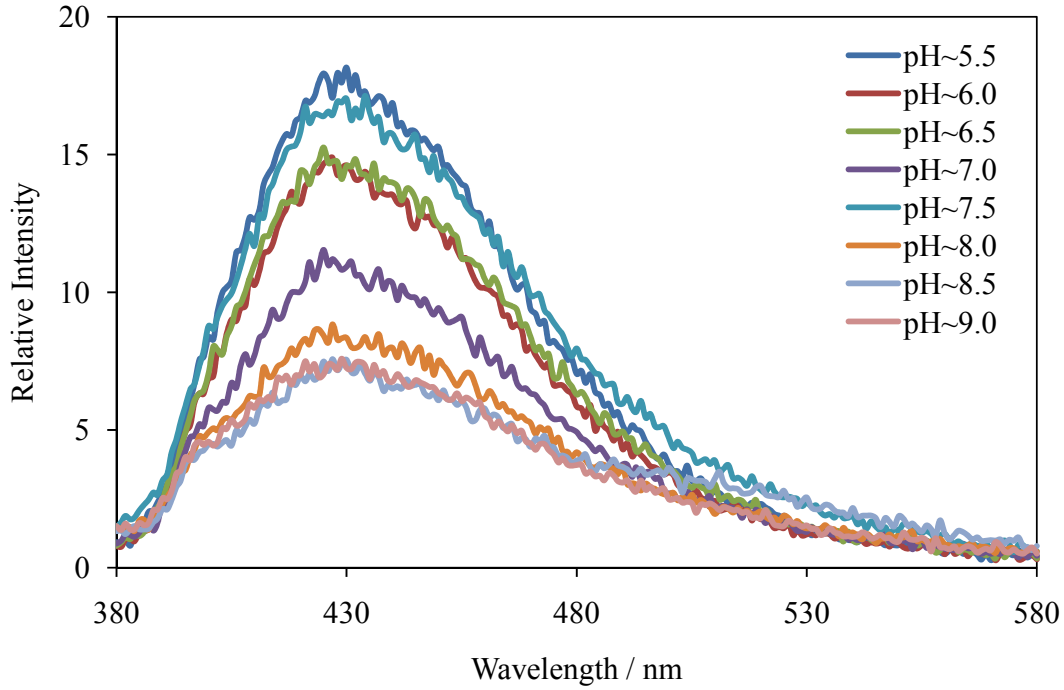

Figure 11: Emission spectra of HSNP sensors excited at λ_{ex} = 350 nm in various pH buffer solutions.

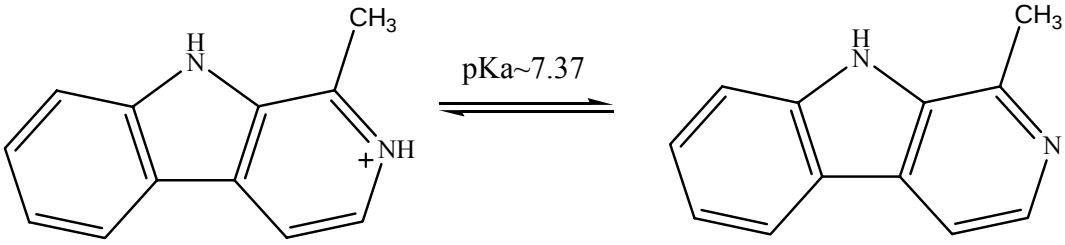

Figure 12: Cationic (emission maximum ca. 430 nm) and neutral (emission maximum ca. 381 nm) species of harmane (Wolfbeis et al., 1982). The pKa value of aromatic heterocyclic nitrogen was reported as 7.37 and the neutral species was reported to be present in the pH range of 8~13 (Wolfbeis et al., 1982)

References

Wolfbeis, O. S., Fürlinger, E., Wintersteiger, R. (1982) Solvent- and pH-Dependence of the Absorption and Fluorescence Spectra of Harman: Detection of Three Ground State and Four Excited State Species. Monatshefte für Chemic 113, 509-517.

Wolfbeis, O. S., Fürlinger, E. (1982) The pH-Dependence of the Absorption and Fluorescence Spectra of Harmine and Harmol: Drastic Differences in the Tautomeric Equilibria of Ground and First Excited Singlet State. Zeitschrift für physikalische chemie Neue Folge Bd. 129, S. 171-183.

Chapter 5: Characterizing fluorescein isothiocyanate (FITC) labeled gelatin nanoparticle (FGNP) sensors

Results

In Fig. 13 and Fig. 14 are shown the fluorescent test results of free FITC and FITC labeled gelatin nanoparticle (FGNP) sensors in various pH buffer solutions from 2.5 to 7.5. In both graphs, the two batches of FGNP sensors at various pH's displayed almost the identical behavior, while free FITC at various pH's exhibited different behavior, especially when pH was below 6.0. In addition, when pH increased from 2.5 to 7.5, both FITC and FGNP sensor fluorescence ratio (peak intensity ratio or peak area ratio) decreased continuously. Although these two curves (for FGNP and free FITC) were not identical, the continuously decreasing fluorescent intensity ratio suggested that FGNP sensors might be a good candidate for pH sensor in food over the range from 2.5 to 7.5.

Discussion

The emission maxima of both FITC and FGNP sensor did not exhibit significant change with pH. Emission spectra of the FGNP sensor are shown Fig. 15 and Fig. 16. However, previous research was shown that fluorescein displays four prototropic forms: cation, neutral, monoanion and dianion with $pKa_l = 2.08$, $pKa_2 = 4.31$ and $pKa_3 = 6.43$ (Yguerabide et al., 1994; Sjöback et al., 1995). FITC almost has the same structure as fluorescein except for the additional isothiocyanate group, so they should share similar protonation and fluorescent properties. The four prototropic forms of FITC are indicated in Fig. 17.

The spectra of the four prototropic forms overlap substantially and the different pKa values are quite close, making the fluorescent properties of FITC relating to the concentrations of these prototropic forms strongly pH dependent. The fluorescent intensity ratio of FITC thus changes continuously as pH changes.

Unlike QSNP and HSNP sensors, which do not significantly change their fluorescent intensity ratio when bound to starch nanoparticles, FGNP sensors are complicated by the presence of acid and base groups, because gelatin nanoparticles contain numerous amine and carboxylic groups. Once FITC was covalently attached to gelatin nanoparticles, it would be influenced by a local buffer system consisting of these amine and carboxylic groups. Hence, the two batches of FGNP sensors displayed different fluorescent intensity ratio against pH curve from free FITC, especially at pH below 6.0. The fluorescent intensity ratio of labeled FITC is smaller than free FITC in the same pH buffer solution; this means that the microenvironment of gelatin nanoparticles' surface where FITC are attached has a lower $[H^+]$ than the solution due to the buffer effect of amino and carboxylic groups on the gelatin nanoparticles. This effect is more apparent at lower pH. But when pH is above 6.5, the effect is very slightly reversed. The microenvironment of gelatin nanoparticles' surface has a very slightly higher $[H^+]$ than the solution and the fluorescent intensity ratio of labeled FITC is higher than for free FITC. This effect is more clearly apparent in the area ratio (Fig. 14) than in the intensity ratio (Fig. 13).

Fluorescein, that is, the parent dye without the isothiocyanate group, was also tried to be labeled onto gelatin nanoparticles. However, after three days dialysis against distilled

water, most fluorescein molecules were removed and the fluorescence signal on nanoparticle was too low to be used to indicate pH.

Conclusion

FITC was covalently used to label gelatin nanoparticles. FGNP sensors and FITC displayed different fluorescence intensity ratios, especially in the low pH range. That's because FGNP sensors are based on gelatin nanoparticles, which are chemically different from QSNP sensors and HSNP sensors based on neutral starch nanoparticles. Because gelatin nanoparticles are more like a small buffer system, labeled FITC will be affected and the signal is different from free FITC. FGNP sensors do not exhibit any apparent emission maximum shifts, but FGNP sensors' peak intensity or peak area ratio did increase continuously as pH increased over the range from pH 2.5 to 7.5, which covers the pH value of most food products, suggesting FGNP sensors may be very good pH sensors for food.

Fluorescein was not successfully labeled onto gelatin nanoparticles. However, fluorescein was proved to be a pH-dependent probe (Sjöback, 1995; Moorthy, 1998). Further study can try to add fluorescein probe into gelatin solution before cross-linking, which perhaps can trap some fluorescein molecules inside gelatin nanoparticles in order to increase fluorescence signal after dialysis.

Tables & Figures

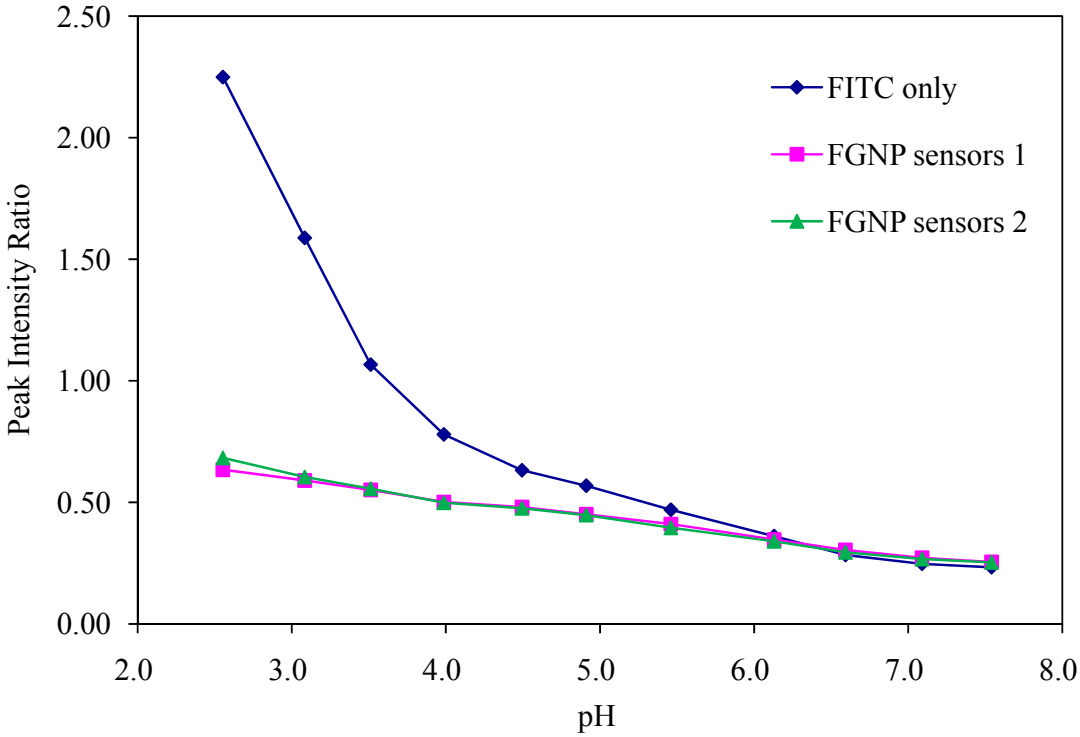

Figure 13: Comparison plot depicting the ratio of peak intensities, $I_{435/460}$, of FGNP sensor (FGNP sensors 1 and FGNP sensors 2 are two batches of FGNP) and FITC solutions at various pH.

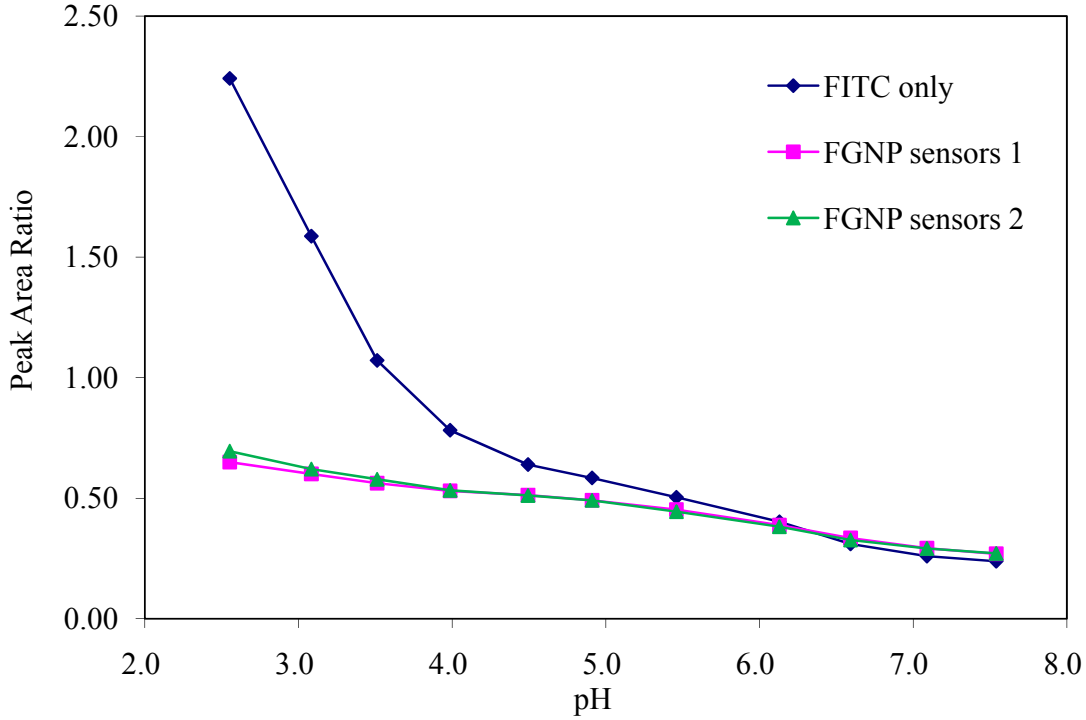

Figure 14: Comparison plot depicting the ratio of peak areas, $A_{435/460}$, of FGNP sensor (FGNP sensors 1 and FGNP sensors 2 are two batches of FGNP) and FITC solutions at various pH.

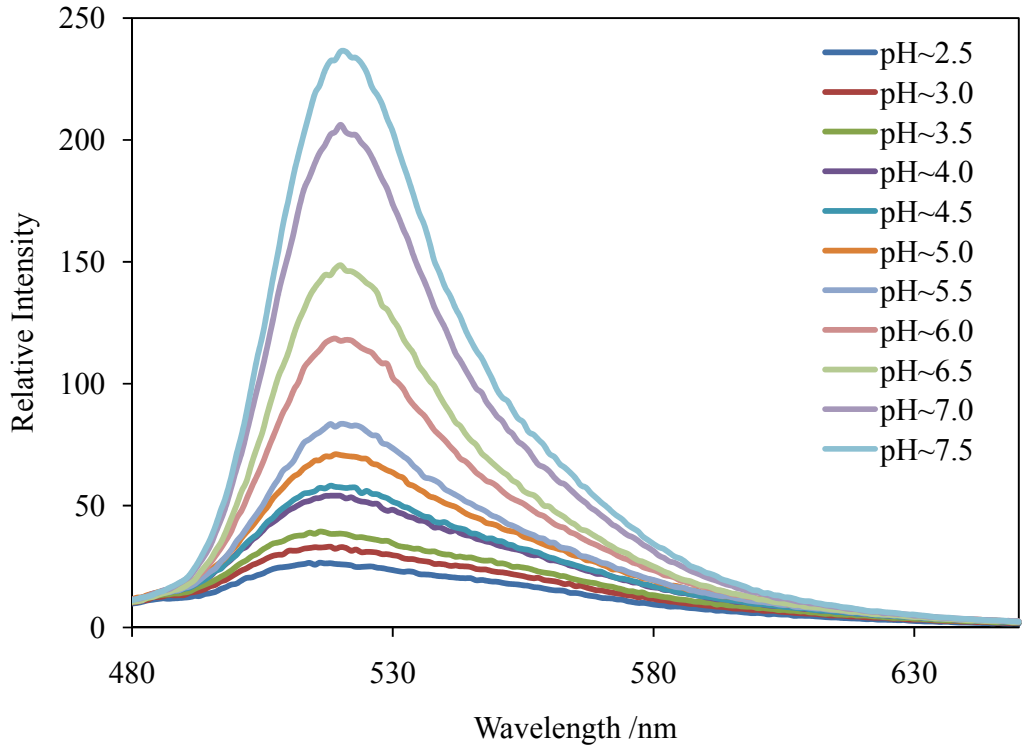

Figure 15: Emission spectra of FGNP sensors excited at λ_{ex} = 460 nm in various pH buffer solutions.

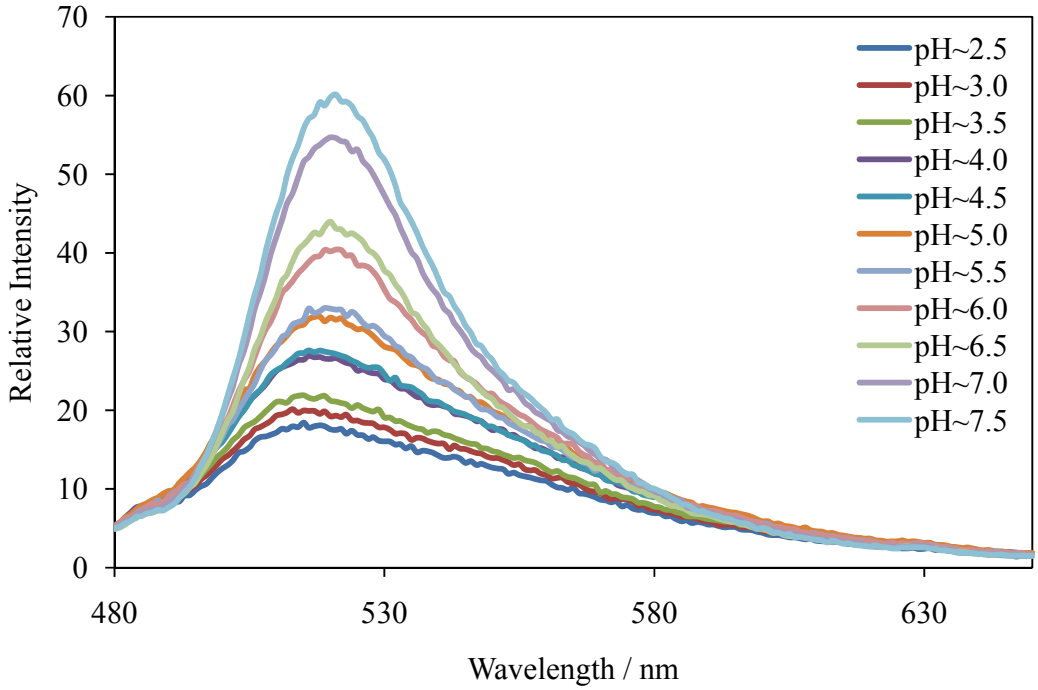

Figure 16: Emission spectra of FGNP sensors excited at λ_{ex} = 435 nm in various pH buffer solutions.

Cation:

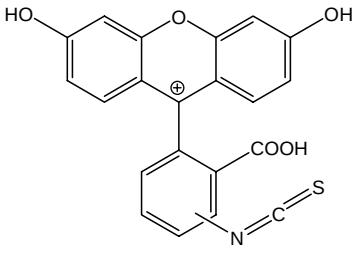

Neutral:

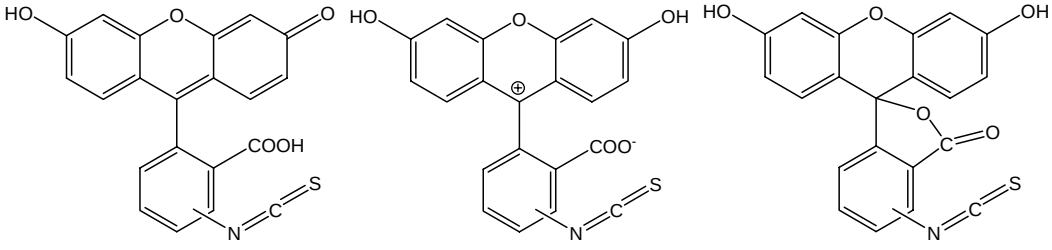

Monoanion:

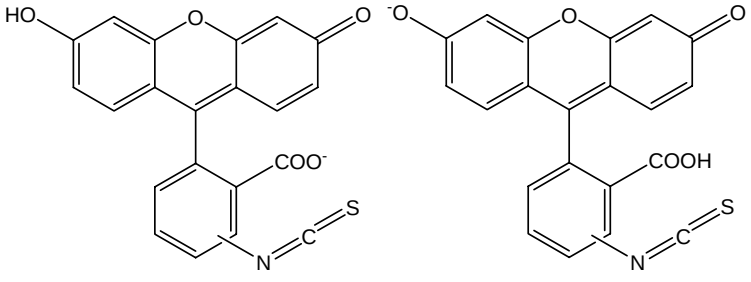

Dianion:

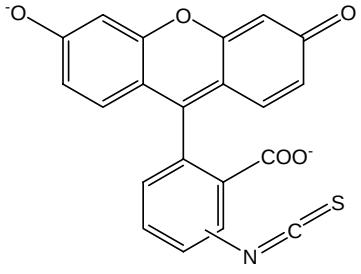

Figure 17: Cation, neutral, monoanion and dianion prototropic forms of FITC (Sjöback et al., 1995).

References

Sjöback, R., Nygren, J., Kubista, M. (1995) Absorption and fluorescence properties of fluorescein. Spectrochimica Acta Part A 51, L7-L21.

Yguerabide, J., Talavera, E., Alvarez, J. M., Quintero, B. (1994) Steady-state fluorescence method for evaluating excited state proton reactions: application to fluorescein. Photochem. Photobiol. 60, pp. 435–441.

Chapter 6: Characterizing FITC labeled gelatin nanoparticle sensors in various food products

Results

Fluorescent tests of FGNP sensors in various food samples

FGNP sensors were tested in several food samples, including Sprite, Orangeade Snapple, Snapple iced tea, Goya® papaya nectar, Hero® guava nectar, Rienzi® pear nectar, several Stop&Shop® canned foods, Tuscan® fat free milk, Kuang®soymilk, Knorr®chicken soup, Stop&Shop® mayonnaise, DANNON® yogurt, Turkey Hill® green tea, Lipton® green tea, Wei-chuan® soy sauce, Tiger Tiger® fish sauce, Marukan® Rice vinegar, Shoprite®grape juice, Bolthouse farms® carrot juice, Wei-chuan® aloe juice, homemade watermelon juice and homemade mayonnaise. FGNP performed well in many of these food samples. For each food sample, its pH value determined using the pH meter is termed meter pH. The fluorescent peak intensity ratio of the food samples was obtained by applying FGNP sensors and then was compared with the FGNP calibration curve, which was developed using the average peak intensity ratios of two batches of FGNP sensors. Each food sample's fluorescent peak intensity ratio could give a pH value based on the calibration curve. This pH value is called sensor pH. In Fig. 18, data are plotted based on fluorescent peak intensity ratio along with FGNP calibration curve against food samples' meter pH. The data of each food sample's meter pH, calculated sensor pH and percentage error of sensor pH compared to meter pH are listed in Table 1. Emission spectra of FGNP sensors in milk and mayonnaise samples are graphed in Fig. 20 and 21, Fig. 22 and 23, respectively.

However, FGNP sensors were not effective all the time. For example, FGNP sensors could not give any detectable fluorescent signal in soy sauce and grape juice, probably because these two solutions are too dark and absorbed all signals. FGNP sensors fluorescence signal was also very weak in yogurt and carrot juice, causing very large and variable errors. When tested in fish sauce, FGNP sensors' fluorescent signal after subtracting the background became negative. The reason is not clear as the ingredients of fish sauce are too complicated. When tested in green tea and iced tea, FGNP sensors aggregated immediately after being added into those tea samples and no fluorescent signal could be detected after that because the sample became too turbid. A possible reason for their aggregation is that tea samples contain a lot of polyphenols, which may cause the positive charged gelatin nanoparticles to be easily aggregated.

Duplicated fluorescent tests of FGNP sensors in different kinds of food samples

Three different kinds of food samples were used to test reproducibility of the fluorescence measurement: sprite, guava nectar and mayonnaise. Sprite is clear and colorless; guava nectar after passing through filter paper would be much clearer than before, but still contain a lot of very small particles and natural pigments; and mayonnaise, different from other liquid food samples tested, is a concentrated stable emulsion. Each sample was tested 5 times using FGNP sensors and the results are listed in Table 2.

Fluorescent tests of FGNP sensors of various concentrations in food samples

Sprite was employed to test the effect of the concentration of FGNP sensors, from 1 mg/ml to 0.1 mg/ml, on the calculated sensor pH. The tests were performed once with concentrations of 0.8 mg/ml and 0.6 mg/ml and were performed twice with concentrations of 0.4 mg/ml, 0.2 mg/ml and 0.1 mg/ml. The results are listed in Table 3.

Discussion

Both FGNP sensors' fluorescent peak area ratio and peak intensity ratio were obtained to generate calibration curves. However, applying the fluorescent peak area ratio in calculating sensor pH always caused larger errors than applying fluorescent peak intensity ratio. Meanwhile, determining peak intensity is much easier than determining peak area. Therefore, fluorescent peak intensity ratio was finally chosen for all food sample studies.

Based on peak intensity ratio, FGNP sensors performed successfully in most real food samples. In Fig. 18, most measurements of the fluorescent intensity ratio are very close to the calibration curve, which means the tested fluorescent intensity ratios are close to the anticipated fluorescent intensity ratio. These fluorescent intensity ratio data were also used to calculate food samples' sensor pH, which is used in Fig. 19 to plot a reference line with sensor pH equal to meter pH. It is clear that most data are very close to or on this line indicating that most food samples' sensor pH was close to the meter pH. In all cases but one, the absolute values of the percentage errors were within ~5%; only vinegar gave higher error.

The results of the fluorescence reproducibility tests of FGNP sensors in three different kinds of food samples demonstrated that FGNP sensors have very good repeatability. The standard deviation of sensor pH was only 0.031 for Sprite, 0.073 for guava nectar and 0.039 for mayonnaise. The average sensor pH was also accurate. For Sprite, the average sensor pH was 3.291, only -0.33% error comparing to the meter pH of 3.302. For guava nectar, the average sensor pH was 3.776; the percentage error of sensor pH was much higher, varying from about 3% to 8% with an average of 6.58% compared to the meter pH of 3.543. For mayonnaise, the average sensor pH was 3.839, a 1.61% error compared to the meter pH of 3.778. These results suggest that there might be a systematic error existing in the guava nectar test as the sensor pH was always higher than the meter pH. It may be because of the small particles in guava nectar's filtrate or the natural pigments in the guava nectar. For mayonnaise, although the results of the reproducibility tests showed all positive errors, negative error did appear sometimes, for instance in Table 1. Hence, the percentage errors of both Sprite and mayonnaise tests just randomly vary around 0.

All the fluorescent test results described above were performed using FGNP sensors at concentration ~1 mg/ml. Based on the description in the methodology section in chapter 2, concentration has nothing to do with the intensity ratio. However, the data in Table 3 clearly showed that at lower concentration of FGNP sensors, the intensity ratio increases. Such phenomena only occured when FITC was labeled onto gelatin nanoparticles. The intensity ratio of free FITC did not change with concentration: 1×10^{-5} M free FITC gave intensity ratios 2.251, 1.537 and 1.071 in buffer solutions (pH 2.5, 3.0 and 3.5, respectively); 1×10^{-6} M free FITC gave intensity ratios 2.289, 1.541 and 1.071 in the same

buffer solutions. The difference between FGNP sensors and free FITC is only because of gelatin nanoparticles. As discussed before, labeled FITC is influenced by gelatin nanoparticles, so the intensity ratio is lower than free FITC at the same condition when pH was below 6. Hence, a possible explanation here is that at lower concentration of FGNP sensors, the gelatin nanoparticles' buffer effect is weakened and labeled FITC now is more influenced by environment pH condition, which causes a higher intensity ratio. To eliminate this error caused by different nanoparticle sensors concentration, an efficient way is to calculate the calibration curve using the same concentration of FGNP sensors as used to test food samples. In one trial, the ~10.50% error was reduced to about ~1% when a calibration curve was plotted based on the data from 0.1 mg/ml FGNP sensors.

Conclusion

Fluorescent tests of FGNP sensors in real food samples showed that sensor pH based on FGNP sensors' peak intensity ratio and calibration curve were very close to the meter pH of food samples under most conditions. Duplicated fluorescent tests showed that the reproducibility of FGNP sensors in food is good, although some system errors exist in particular samples. Further research may be conducted to clarify the system error. The concentration of FGNP sensors used to plot calibration curve should be the same as the concentration used to test food samples to obtain the best results, otherwise much higher error may occur. In general, these results suggest FGNP sensors may be very good pH sensors, sufficiently precise and accurate for use in food.

Tables & Figures

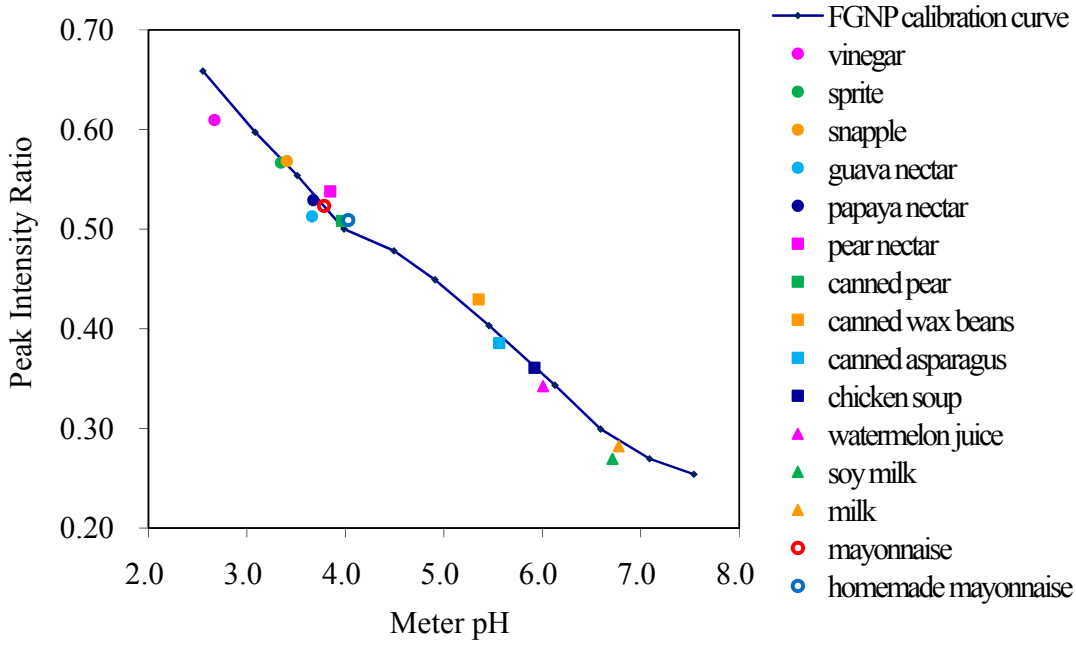

Figure 18: Comparison plot depicting the ratio of peak intensity, $I_{435/460}$, of FGNP sensors and FGNP calibration curve as a function of pH in various food products.

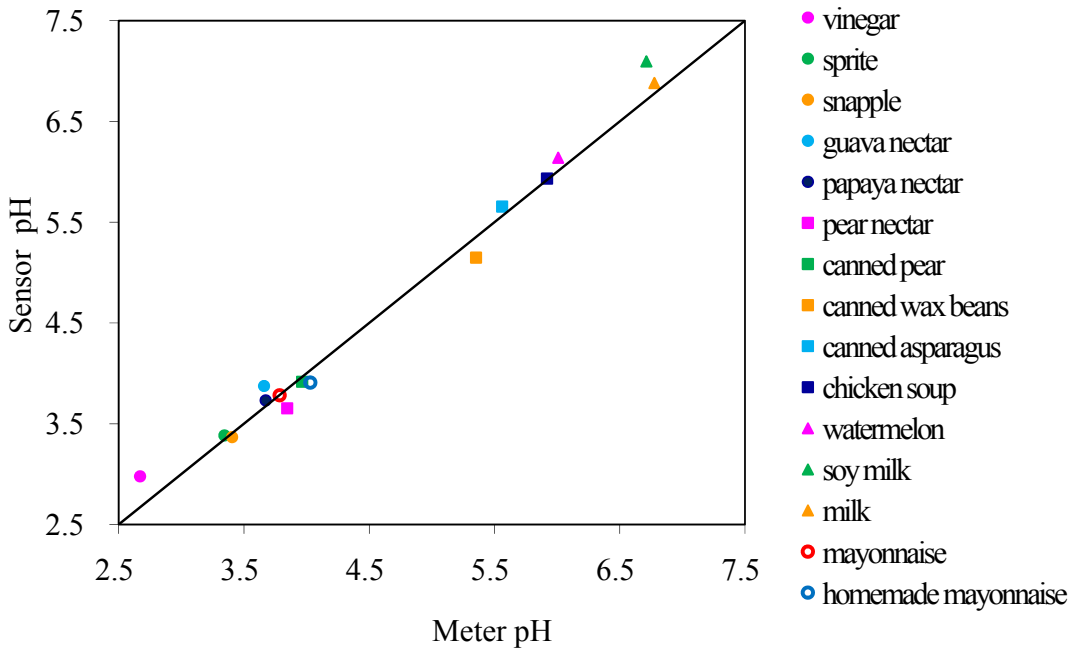

Figure 19: Comparison plot depicting the sensor pH of food products determined by peak intensity ratio using FGNP calibration curve against meter pH.

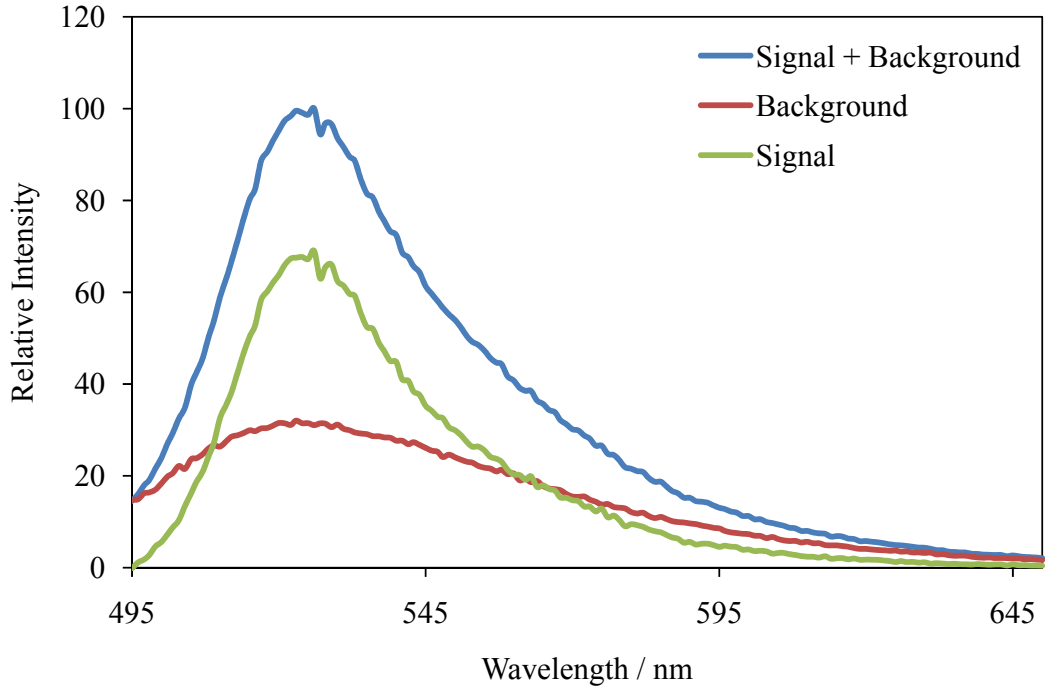

Figure 20: Fluorescence tests of FGNP sensors in milk, excited at λ_{ex} = 460 nm. Blue line is fluorescence signal of FGNP sensors in milk + milk background. Red line is milk background only. Green line = Blue line – Red line is the fluorescence signal of FGNP sensors in milk.

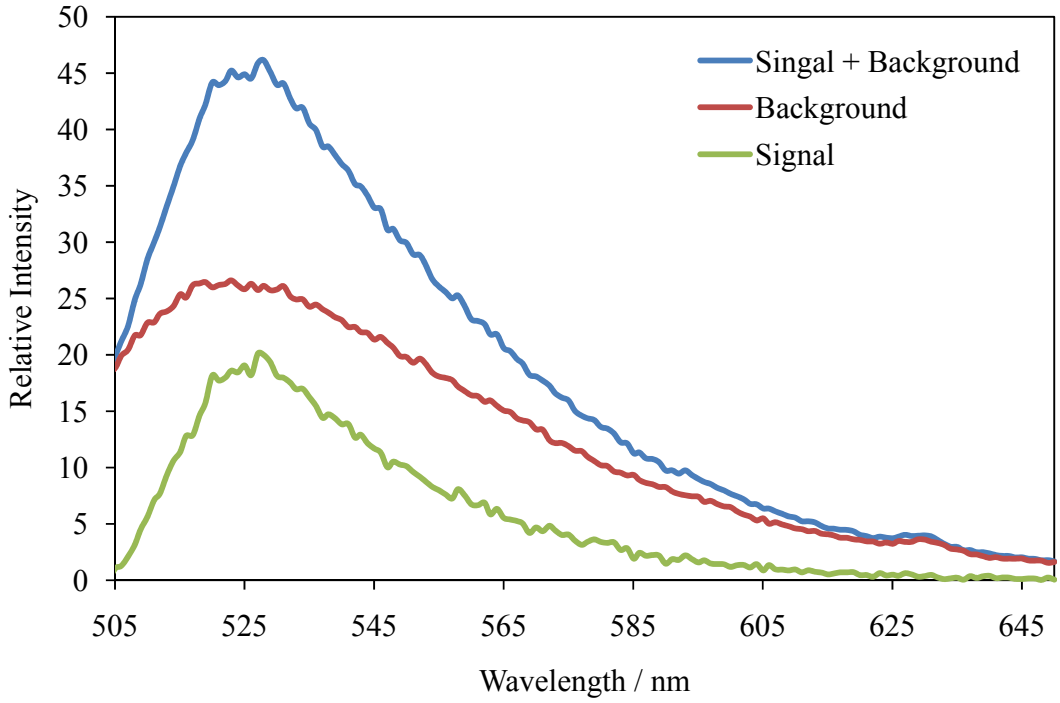

Figure 21: Fluorescence tests of FGNP sensors in milk, excited at λ_{ex} = 435 nm. Blue line is fluorescence signal of FGNP sensors in milk + milk background. Red line is milk background only. Green line = Blue line – Red line is the fluorescence signal of FGNP sensors in milk.

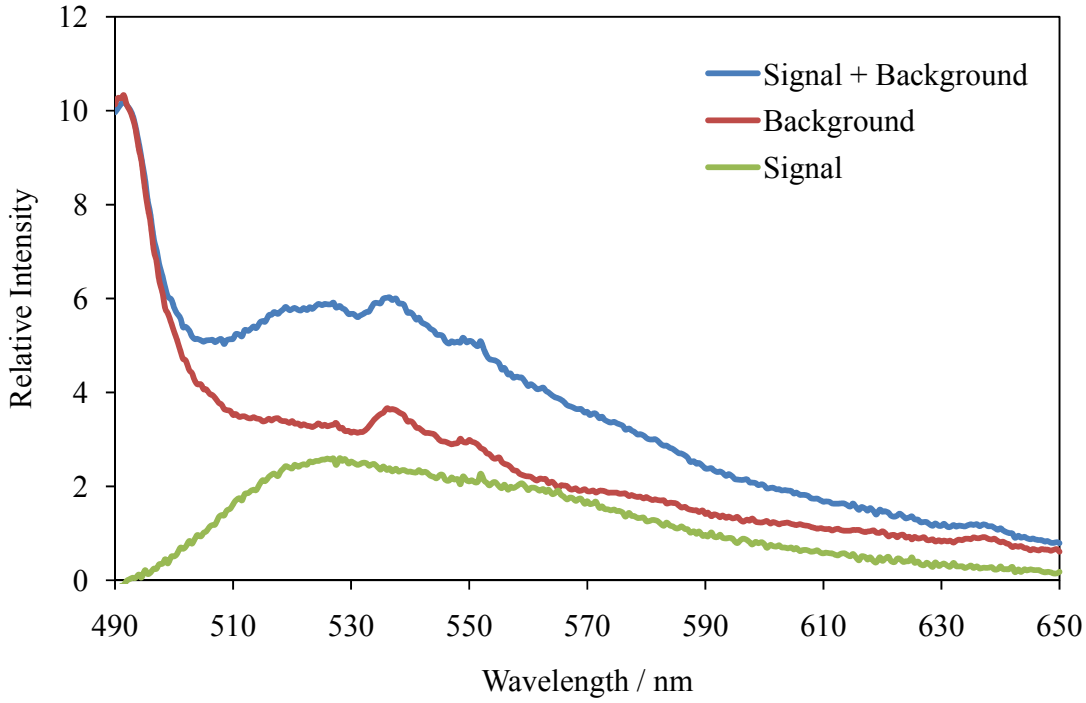

Figure 22: Fluorescence tests of FGNP sensors in mayonnaise, excited at λ_{ex} = 460 nm. Blue line is fluorescence signal of FGNP sensors in mayonnaise + mayonnaise background. Red line is mayonnaise background only. Green line = Blue line − Red line is the fluorescence signal of FGNP sensors in mayonnaise.

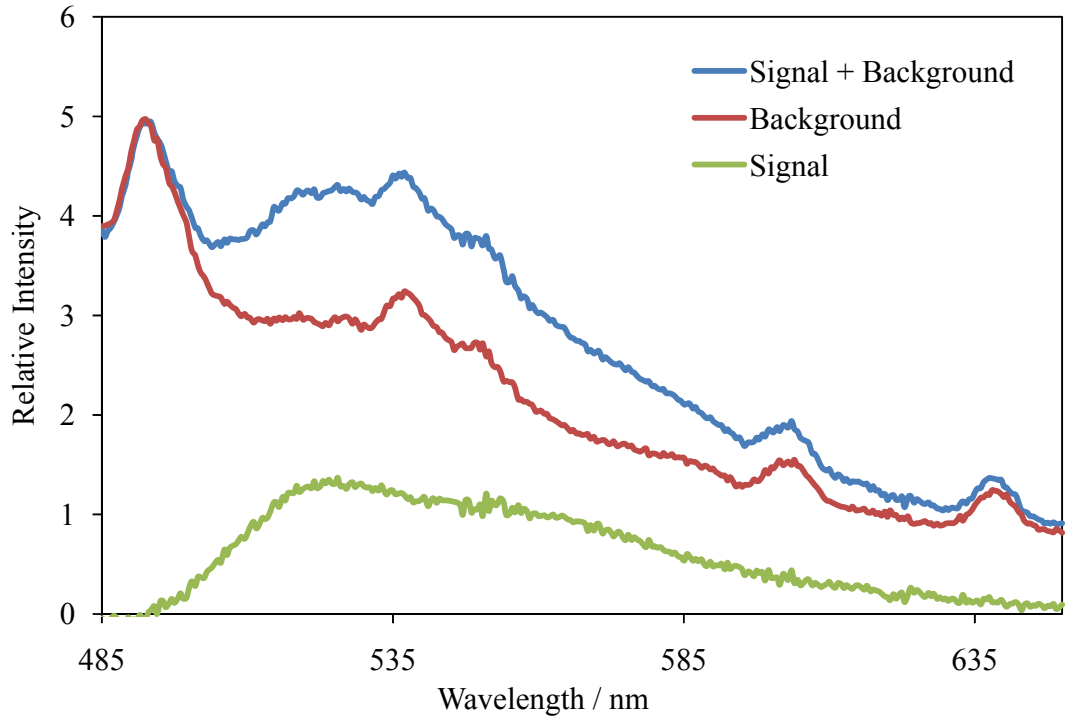

Figure 23: Fluorescence tests of FGNP sensors in mayonnaise, excited at λ_{ex} = 435 nm. Blue line is fluorescence signal of FGNP sensors in mayonnaise + mayonnaise background. Red line is mayonnaise background only. Green line = Blue line − Red line is the fluorescence signal of FGNP sensors in mayonnaise.

Food Product	Meter pH	Sensor pH	Percentage Error
vinegar	2.671	2.979	11.53%
sprite	3.345	3.385	1.20%
snapple	3.406	3.368	-1.12%
guava nectar	3.661	3.875	5.85%
papaya nectar	3.674	3.732	1.58%
pear nectar	3.846	3.654	-4.99%
canned pear	3.965	3.917	-1.21%
canned wax beans	5.353	5.148	-3.83%
canned asparagus	5.562	5.655	1.67%
chicken soup	5.920	5.933	0.22%
watermelon	6.009	6.140	2.18%
soy milk	6.713	7.095	5.69%
milk	6.777	6.881	1.53%
mayonnaise	3.785	3.783	-0.05%
homemade mayonnaise	4.030	3.909	-3.00%

Table 1: Percentage error of food samples' sensor pH compared to meter pH.

Food Product	Meter pH	Sensor pH	Percentage Error
Sprite	3.302	3.269	-1.01%
		3.335	1.01%
		3.293	-0.28%
		3.285	-1.34%
		3.275	-0.83%
guava nectar	3.543	3.650	3.02%
		3.813	7.62%
		3.836	8.26%
		3.793	7.04%
		3.786	6.87%
mayonnaise	3.778	3.864	2.27%
		3.889	2.93%
		3.841	1.67%
		3.803	0.67%
		3.796	0.49%

Table 2: Reproducibility fluorescent tests results of FGNP sensors in three food samples. The meter pH's are not the same as they appear in Table 1 because they were not obtained on the same day.

Food Product (Concentration of FGNP)	Meter pH	Intensity Ratio	Sensor pH	Percentage Erro
Sprite (1 mg/ml)	3.302	0.5785	3.269	-1.01%
Sprite (0.8 mg/ml)		0.5829	3.225	-2.32%
Sprite (0.6 mg/ml)		0.5833	3.222	-2.42%
Sprite (0.4 mg/ml)		0.5867	3.189	-3.44%
Sprite (0.4 mg/ml)		0.5870	3.185	-3.54%
Sprite (0.2 mg/ml)		0.5975	3.081	-6.68%
Sprite (0.2 mg/ml)		0.5934	3.122	-5.44%
Sprite (0.1 mg/ml)		0.6009	3.048	-7.69%
Sprite (0.1 mg/ml)		0.6103	2.955	-10.50%

Table 3: Fluorescent tests results of FGNP sensors at various concentrations in Sprite.

Chapter 7: Efforts characterizing water activity-sensitive probes

Materials and Methods

Materials

Lithium chloride, potassium acetate, magnesium chloride, potassium carbonate, magnesium nitrate, sodium bromide, sodium chloride, potassium chloride, Prodan, Laurdan and glycerol were purchased from Sigma-Aldrich and used as purchased.

Preparation of solutions

Saturated salt solutions were prepared simply by adding excess salt into distilled water (Greenspan, 1977). All salt solutions were then well shaken and stored at room temperature overnight to reach equilibrium. Water-glycerol solutions with different mass fraction of glycerol were prepared based on Ninni et al. (2000) and stored at room temperature. Prodan was dissolved in DMF to prepare a 20 mM stock solution and stored in a refrigerator. Laurdan was dissolved in DMF to prepare a 20 mg/ml stock solution and stored in a refrigerator. Laurdan does not completely dissolve in DMF, so the concentration of stock solution was lower than 20 mg/ml. Most attention was directed to fluorescent emission spectra shifts, so the exact concentration of probe is not important in this study.

Methodology & Fluorescent measurements of Prodan and Laurdan

As mentioned in Chapter I, Prodan and Laurdan are expected to present emission maximum shifts under different water activity conditions. Hence, the effects of concentration should be eliminated, which may vary among trials. When conducting fluorescent tests, 11.4 μL Prodan stock solution was diluted in 5 ml distilled water to 4.6 $\times 10^{-5}$ M. 17.7 μL Laurdan stock solution was diluted in 5 ml distilled water to 2×10^{-4} M in distilled water (the actual concentration would be lower than that, because Laurdan was not completely dissolved in DMF). Then, 150 μL diluted probe solution was then added into cuvette and 2850 μL saturated salt solution or water-glycerol solution was added. (Here, when saturated salt solutions or water-glycerol solutions were added into the cuvette, they were diluted by probe solution. However, the volume of probe solution is only one twentieth of the volume of final solution. It may change the water activity of saturated salt solutions or water-glycerol solutions, but the influence will be limited and will not change the qualitative results.) The final concentration of Prodan and Laurdan was 2.3×10^{-6} M and 1×10^{-5} M, respectively. A small stir bar was put into the cuvette to help mix samples. The cuvette was then incubated in a constant temperature holder in the Cary Eclipse fluorescence spectrophotometer at 25 ℃. Both Prodan and Laurdan were excited at 360 nm. Data were collected every 10 minutes after samples were mixed.

Results & Discussion

Prodan

In Fig. 25 are shown the emission spectra of Prodan in water and different saturated salt solutions. As the water activity changed, the emission spectrum of Prodan changed spontaneously. However, it is hard to find any relation between water activity and emission maxima of Prodan. As shown in Table 4, the emission maxima of Prodan changed little in the water activity range from 0.5 to 1.0. But as the water activity decreased from ~0.53 to ~0.43, the emission maximum blue-shifted about 100 nm. The results indicate that the shifts of emission spectra of Prodan may not be simply related to water activity. Other factors such as charge species, ion charge density and ion species may also play an important role in affecting the emission maxima of Prodan.

We also find that the emission spectra of Prodan have two peaks in Fig. 25. One low energy emission has maximum at about 525 nm; the other high energy emission has maximum at about 420 nm. The intensity ratios of $I_{525/420}$ are listed in Table 5 with water activities. Unfortunately, there is still no relation between the $I_{525/420}$ and the water activity.

To simplify the problem, water-glycerol systems with different mass fraction of glycerol were employed and investigated. The relation between mass fraction of glycerol and water activity is listed in Table 6 (Ninni et al., 2000). In Fig. 26 are shown the emission spectra of Prodan in water-glycerol solutions of different water activity. As the water activity decreased from 1.0 to 0.40, the fluorescent intensity increased. However, there were no apparent emission maxima shifts and the fluorescent intensity was influenced by probe

concentration, which can hardly be controlled constant among trials. Therefore, the results of Prodan in water-glycerol systems also indicate that Prodan may not be a good candidate for indicating water activity.

In addition, there is another aspect of the Prodan experiments, which also limited the application of Prodan as a water activity probe. In both saturated salt and water-glycerol experiments, data were collected every 10 minutes after samples were mixed. 10 minutes are supposed to be enough for samples to reach temperature equilibrium and water activity equilibrium in solutions. However, in many cases, Prodan displayed intensity increases at 20 minutes or 30 minutes or even longer after the samples were mixed. These results suggest that Prodan cannot reach equilibrium in a short time in these solutions.

Laurdan

Laurdan has the same structure as Prodan except for the presence of a long carbon chain (Fig. 24). Although Laurdan was excited at 360 nm, the same wavelength as Prodan, their emission spectra are different. As shown in Fig. 27, only distilled water and three other saturated salt solutions were tested. The fluorescent intensities decrease as the water activity of the solutions decrease from nearly 1.0 (water) to about 0.33 ($MgCl_2$). But once again, almost no emission maximum shift was observed. All experiments were conducted at 25 ℃ and data were collected 20 mins after samples were prepared.

Conclusion

Both Prodan and Laurdan were tested as water activity probes. The fluorescence intensity of Laurdan decreased as the water activity of the saturated salt solutions decreased. However, Laurdan did not display any apparent emission maximum shifts at all. Prodan did display emission maximum shifts in various saturated salt solutions, but there is no evidence that these emission maximum shifts correspond to water activity and can be used to indicate water activity. The emission maximum shifts may be due to other factors such as charge species, ion charge density and ion species. To eliminate these effects, various concentrations of water-glycerol solutions were tested. Prodan in water-glycerol solutions showed that the fluorescence intensity increased when water activity of the solutions decreased. However, there were no apparent emission maximum shifts displayed by Prodan in various water-glycerol solutions. Because fluorescence intensity is probe concentration dependent which can hardly be controlled constant among trials, fluorescence intensity alone thus cannot be used as a standard to indicate water activity. In addition, Prodan does not reach equilibrium quickly in either salt solutions or water-glycerol solutions. Equilibrium takes 20 minutes or more depending on the solute. Therefore, these results indicate that Prodan and Laurdan are not good candidates as indicators of water activity.

Tables & Figures

	Water Activity	Emission maxima
Lithium Chloride	0.1130	~420 nm
Potassium Acetate	0.2251	~509 nm
Magnesium Chloride	0.3278	~417 nm
Potassium Carbonate	0.4316	~434 nm
Magnesium Nitrate	0.5289	~536 nm
Sodium Bromide	0.576	~536 nm
Sodium Chloride	0.7529	~532 nm
Potassium Chloride	0.8334	~528 nm
Water	1.0	~526 nm

Table 4: Water activity of various saturated salt solutions. The middle column is the water activity of different saturated salt solutions (Greenspan, 1977) in water at 25 ℃. The right column is the emission maxima of Prodan in each solution.

	Water Activity	$I_{525/420}$
Lithium Chloride	0.1130	6.0442
Potassium Acetate	0.2251	0.2077
Magnesium Chloride	0.3278	4.1008
Potassium Carbonate	0.4316	5.4935
Magnesium Nitrate	0.5289	0.2365
Sodium Bromide	0.576	0.9537
Sodium Chloride	0.7529	0.7086
Potassium Chloride	0.8334	0.4019
Water	1.0	0.0211

Table 5: Water activity and Prodan $I_{525/420}$ of various saturated salt solutions at 25 ℃.

Mass Fraction of Glycerol	Water Activity
0.1999	0.952
0.3994	0.872
0.5491	0.775
0.6495	0.683
0.7489	0.557
0.7986	0.483
0.8487	0.399

Table 6: Water activity of water-glycerol solutions as a function of mass fraction of glycerol at 25 ℃ (Ninni et al., 2000).

Prodan: **Laurdan:**

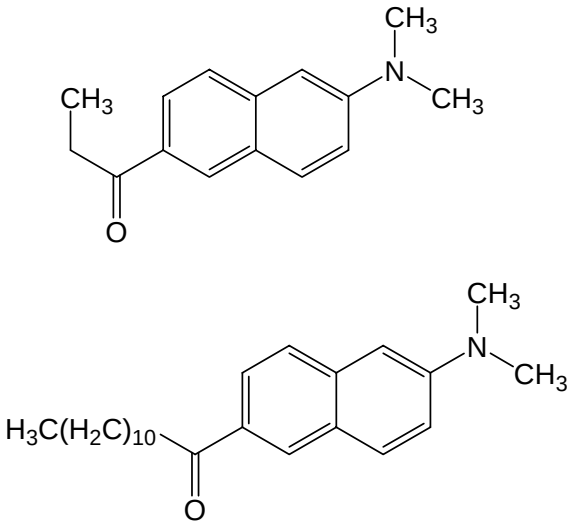

Figure 24: Chemical structure of Prodan and Laurdan.

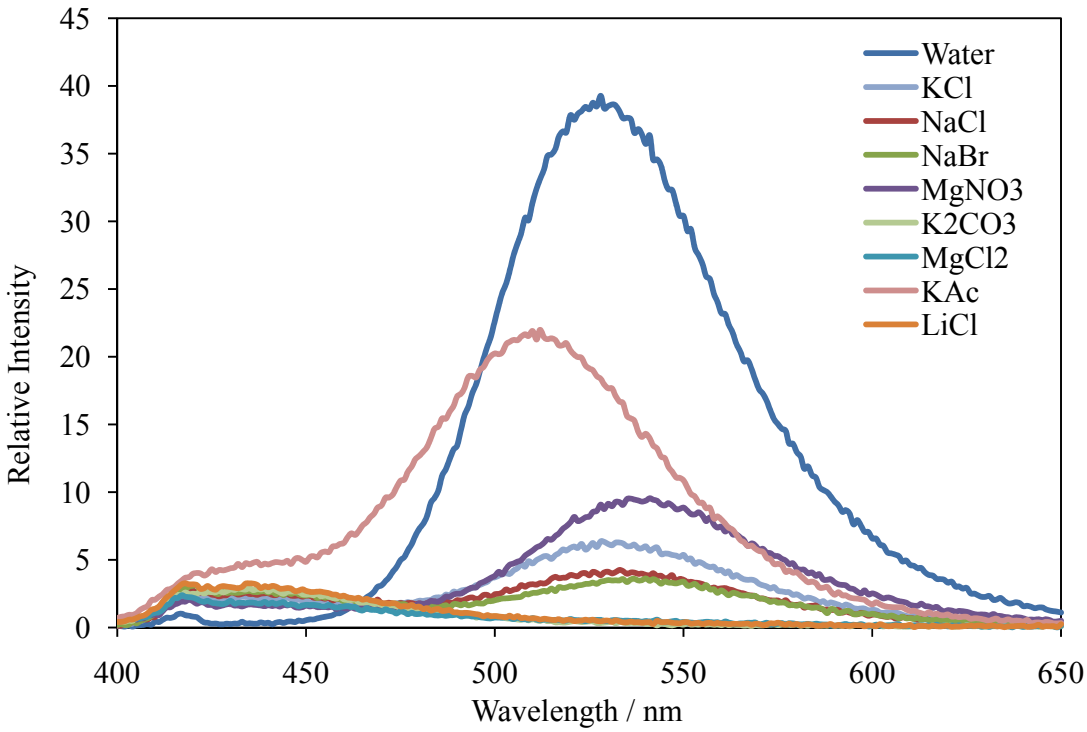

Figure 25: Emission spectra of Prodan in saturated salt solutions. The water activity decreases in the salts listed from top to bottom. Prodan was excited at 360 nm and all data were collected 20 mins after Prodan was mixed with the saturated salt solution. Experiments were conducted at 25 ℃.

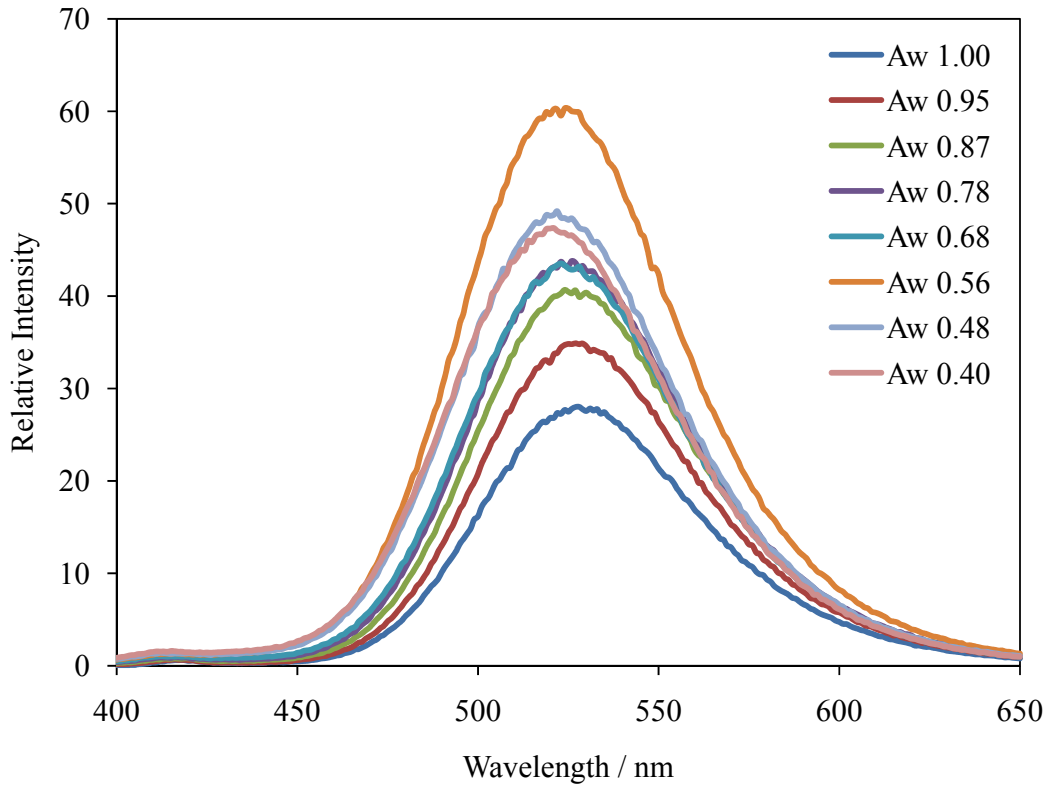

Figure 26: Emission spectra of Prodan in water-glycerol solutions of different water activity. Prodan was excited at 360 nm and all data were collected 20 mins after Prodan was mixed with water-glycerol solution. Experiments were conducted at 25 ℃.

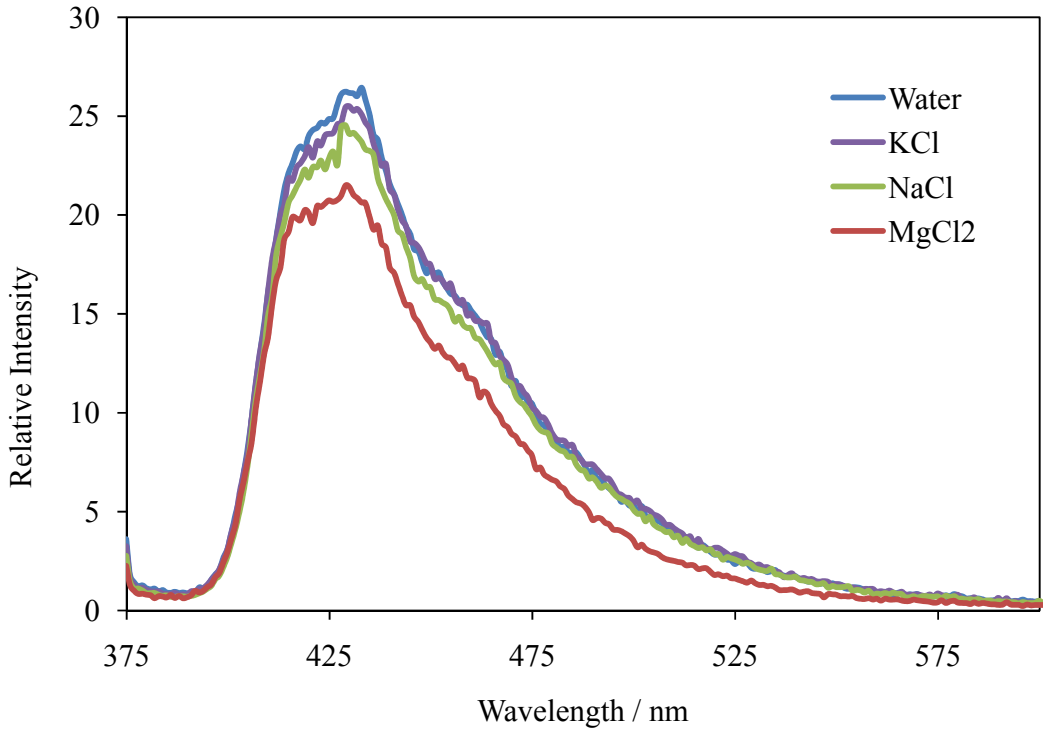

Figure 27: Emission spectra of Laurdan in water and saturated salt solutions of different water activity. Water activity decreases for the solutions listed from top to bottom. Laurdan was excited at 360 nm and all data were collected at 20 mins after Laurdan was mixed with water or salt solutions. Experiments were conducted at 25 ℃.

Reference

L. Greenspan. (1977) Humidity Fixed Points of Binary Saturated Aqueous Solutions. J. res. Nat. Bur. Stand. Sect. A. Phys. chem. Vol. 81 A, No. 1, 89-96

L. Ninni, M. S. Camargo, Antonio J. A. Meirelles. (2000) Water Activity in Polyol System. J. Chem. Eng. Data, 45(4), 654-660